Feedback Control of Multiple Machines using Narrowband Power Line Communication

CARRIZO Cesar

Feedback Control of Multiple Machines using Narrowband Power Line Communication

CARRIZO Cesar
Department of Electrical Engineering
and Computer Science,
Graduate School of Engineering,
Nagoya University
2015

Contents

List of figures

List of tables

Chapter 1

Introduction

1.1 Background

Communications for control is by itself a novel concept, since classic control theory considers the connection between the controller and the object that must be controlled, the plant, as ideal. In the case of electronic control systems for example, this is mainly due to the usually neglectable distance between these two elements. The controller which is the device in charge of regulating the input to the plant to obtain a desired output from it, may be connected to the plant in an open or in a closed loop. The latter is the case of a feedback control system. In electronic systems, these loops are in reality communication channels in which disturbances such as noise and interference can occur. These disturbances may corrupt the information being transmitted between the controller and the plant, thus impairing the capacity to effectively control the output of the plant.

Nowadays a wide availability of communication networks provides an ideal setting for studying the interactions of control and communication. There are two approaches to this issue, one is to view it as the way in which the communication channels in the feedback control loop affect the feedback performance and the other is to see how the feedback can affect the communication schemes [1]. In this work the first approach will be focused since the main

interest of this work is the improvement of performance of the system being affected by channel errors.

In physical terms, the communication channels joining the controller and the plant may be a set of dedicated cables, which is the most common case, or wireless channels, among others. Recently there is a growing interest in wireless control because of its ease of implementation and scalability and relative low cost. However due to the unreliable and unpredictable nature of wireless channels, this technology has not become so widespread in critical control applications. Another alternative which is the one explored throughout this work is that of existing power lines inside buildings and all over the public electric grid. The existence of this infrastructure provides a resource that can be used to transmit information and further develop machine-to-machine control (M2M) for factory automation and the future smart grid. Power lines, the fundamental and most widespread energy transfer media in the world, have been used as a means of data transmission since the early 1900s [2]. Recently there is a renewed interest in their use to transmit control signals, to aid in the development of smart grid and industrial environments. The smart grid is a modernized version of the present electric grid and it considers the bidirectional flow of energy as well as intelligent metering and monitoring of the whole infrastructure. The smart grid also includes the addition of renewable energy sources which usually tend to be very variable and make conditions in the grid unstable. To be able to manage the flow of energy in the grid, management of the flow of data is vital. Reliability in the communication of control and sensing signals is necessary for the realization of the future smart grid [3]. The wide availability of power distribution lines makes power line communications (PLC) very appropriate for control applications [4]. In this study power lines as thought as a complement for wireless and dedicated cabling in the transmission of control signals. Among the wireline alternatives, PLC is the only technology with a deployment cost comparable to wireless communications since the power lines are already there [2].

Power line communications can be divided into two main categories, broadband power line communications and narrowband power line communications. Broadband PLC makes use of a wider portion of the electromagnetic spectrum than narrowband PLC, thus higher transmission speeds are possible. However, broadband PLC has a potential to interfere with other communication systems and its short range of communication limits it to indoor use. Narrowband PLC on the other hand, uses a thinner portion of the electromagnetic spectrum; therefore data transmission may be rather slow. However, narrowband PLC also has a lower potential for interference with other systems and its longer propagation range makes it more suitable for outdoor use than broadband PLC.

Aside from the spectrum usage and interference considerations, PLC possesses another remarkable feature and that is the somewhat deterministic cyclostationary nature of its noise and attenuation. Taking this fact into consideration, communication and control schemes of predictive nature may be applied to improve the overall performance of a PLC system. In PLC both noise and attenuation have cyclostationary features, therefore the signal-to-noise ratio (SNR) and the bit error rate (BER) are also cyclostationary [38],[6].

Past studies on control by PLC consider lighting systems with various power line network topologies and transmission methods [4], the transmission of data signals in an environment in which pulse width modulation is used to control a motor [5]. In [38], the authors focused on the behavior of cyclostationary channels in contrast to stationary channels when dealing with a feedback control system. In [4],[5] the influence of errors caused by the noise in the power line and a method to overcome these errors and improve the quality of control had not been considered.

This work considers a feedback loop control system with a rotary inverted pendulum as a plant. A power line is employed as the feedback loop connecting the controller to the controlled object and narrowband PLC is considered. First, the interactions between the characteristic cyclostationary noise in the

narrowband power line environment of the feedback loop and the transmission rate of control signals is explored. As the second step in this research, a measure to improve control quality for a single machine (single plant) under a narrowband power line environment is presented. Later on an extension into a multiple-machine (multiple plants) narrowband power line environment is introduced.

1.2 Purpose of this research

In a feedback control system, specifically, there exists a so called feedback loop between the controller and the plant. Under ideal conditions, the commands sent from the controller to the plant and the state information transmitted from the plant to the controller are considered to be undisturbed and uncorrupted by the channel, therefore error detection and correction techniques typically considered in communication theory are disregarded. In real world conditions, however, disturbances occurring in the feedback loop (the communication channels) and in the plant itself may corrupt the control commands and deteriorate the overall performance of the system. From the viewpoint of control theory, improvements in the controller to consider disturbances in the system may help improve the performance, however these measures may not suffice and the need to consider communication theory techniques may be neccessary for optimization. This work makes use of a simple control system and intends to perform optimizations from the viewpoint of communication theory and by observing the neccessities of the plant.

In previous research, the influence of the cyclostationary noise in narrowband PLC on digital control signals or methods to improve control quality have not been considered. Therefore, initially this research work attempts to clarify how the narrowband power line channel features influence the performance of a feedback control system that employs a power line as a feedback

loop. To assess the influence of the narrowband power line environment on the system, the single machine system considering noise in the power line is compared against an equivalent system with stationary noise.

As mentioned before, due to the somewhat deterministic nature of PLC, a control scheme of predictive nature may be applied. In the current research, one controlled object and one controller, connected to each other through a power line are considered for the single machine case. For the case of a single machine (single plant), this thesis suggests a predictive control scheme to take advantage of high SNR instants to send additional predicted data to be utilized during low SNR instants. The predicted data calculation is based on the mathematical model of the controlled system. In PLC high and low probability of errors occur in a cyclic non-bursty fashion, therefore in this study predictive control is applied to combat single information packet errors. Predictive control for the case in which burst errors (multiple-packet errors) occur in the channel is analyzed in [7].

The control quality of the system, or in other words the ability to keep the plant stable as well as accurate in following desired values for its output, is used to evaluate the performance of the system. A rotary inverted pendulum has been chosen as an example of a plant due to its popularity as a generic representation of an object that requires continuous feedback control [8].

Additionally, a method to improve the control quality and offer fair medium access to multiple machines (multiple plants) in the system is introduced. The multiple machine case considers one controller connected to multiple machines through power lines.

Such a system is considered to have an application in the industry and the smart grid and serve as an alternative and a complement to wireless control and dedicated cable (wired) systems.

1.3 Structure of this thesis

This work is organized in the following manner. In chapter 2 the basic definition of feedback control and the way in which signals are transferred in the channel are presented. In chapter 3 the narrowband power line features considered in the system model are explained. In chapter 4 the influence of errors caused by the noise in the power line on the control quality is presented and backed by some numerical results. Chapter 5 presents a method to improve control quality for a single machine by exploiting the cyclic features of the power line communications. Chapter 6 introduces the concept of multiple machines in the system and proposes an access method to assure fairness. To finalize, in chapter 7 the author presents the summary of the whole work.

Chapter 2

Feedback control overview

Feedback control is basically defined as a control system that examines the process being carried out and makes changes in order to improve the output of the system. The usual objective of such a system is to control the plant output to make it follow a desired control signal input. For the control system considered in this work, an additional element, the communication channels between the controller and the plant are also being considered. For the ease of application of digital processing techniques, discrete-time control is considered instead of continuous-time control. This will be shown in more detail in Chapters 4, 5 and 6.

In the following sections the main elements of the feedback control system being considered will be explained. The power line communication channel will only be mentioned in this Chapter and will be further explained in Chapter 3.

2.1 Basic system structures

The elements of the feedback control system are a controlling terminal (controller), sensors and a controlled object (plant). There are many possible models, some of them considering more than one controller and/or plants, but in

this Chapter the simplest arrangement, which has one controller and one plant, is focused.

For the controlled system the following two arrangements can be considered. In Fig. 2.1 control information is sent from the controller and the control is automatically performed on the plant. The control information sent from the controller can be for example a specific target value or an ON/OFF signal for the controlled object. In this case the controller does not get a feedback from the plant, it simply regulates the input to the plant in some predetermined fashion.

The other system form is shown in Fig. 2.2. In this system there is a feedback loop between the controller and the plant. In such systems the control information is sent to the plant, then information from the plant is measured by the sensor and sent back to the controller. The decisions made at the controller are based on the measurements sent from the sensor and the user-dependent input information. The controller may integrate information from various sensors and various plants. Throughout this work such a feedback control system is considered.

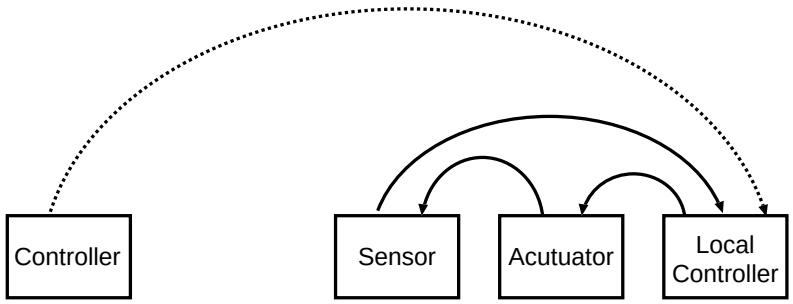

Figure 2.1 Semi-closed loop control system

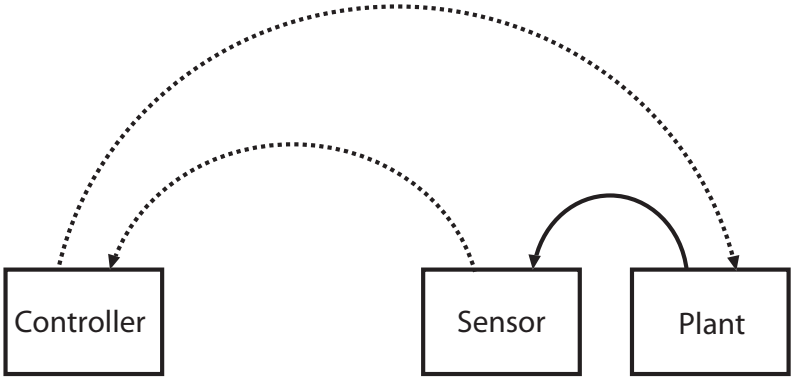

Figure 2.2 Closed loop control system

2.2 Feedback control system

The general scheme of a feedback control system is shown in Fig. 2.3. The target or reference value **r** is a user-defined value input to the controller. Then, from the state information **x** and the control output **y**, the approximated control input **u** is calculated and sent to the plant.

At the plant, the control is carried out according to the control information input **u**, and the control output **y** is measured. After this the state information **x** is fed back to the controller. In this work **y** will generally be considered to be the same as **x**.

The feedback control system considered in this work is assumed as non-ideal, therefore disturbance in the feedback loop, such as channel noise, denoted as $\mathcal{N}$, and the disturbance in the plant, denoted as **w**, must be taken into account.

Disturbance in the channel can corrupt the information being transmitted between the controller and the plant. The way in which this happens is shown in Fig. 2.3 as the control input **u** and the state information **x** become $\breve{\mathbf{u}}$ and $\breve{\mathbf{x}}$ respectively.

$$\breve{\mathbf{u}} = \mathbf{u} + \mathcal{N} \tag{2.1}$$

$$\check{\mathbf{x}} = \mathbf{u} + \mathcal{N}. \tag{2.2}$$

Eq. (2.1) and Eq. (2.2) show how the disturbance affects the information signals being transmitted. In the ideal channel case where there are no disturbances, $\mathcal{N} = 0$. If $\mathcal{N}$ is additive white Gaussian noise, then this represents the wireless channel case. The wireless channel case was studied in [9] and [10]. The case in which $\mathcal{N}$ is cyclostationary noise represents the power line channel which is studied in this work. This will be further explained in Chapter 3.

Disturbance in the plant affects measurements made by sensors for example or may include external disturbances such as vibrations in a mechanical system for example. In this system, plant disturbance is modeled as additive white Gaussian noise.

2.2.1 System performance evaluation

Generally, the performance of a control system is evaluated by determining whether the output of the system settles at a certain value or whether it reaches a steady state after a certain amount of time. System instability may occur even if disturbances are not present in the system. Stability in control engineering is a necessary condition, meaning that it must be maintained for the system to be of practical use. In control theory, there are different types of stability, however this work deals with bounded-input bounded-output (BIBO) stability. BIBO stability refers to a system in which the output signal is bounded for every input signal that is bounded. It is said that a signal is bounded if there is a certain finite value that the signal magnitude never exceeds.

Evaluations based on the difference between the control output $\mathbf{y}$ in the absence and presence of disturbance, such as the root mean square error (RMSE) between these two values, are commonly employed to rate the accuracy of the system and will also be considered in this work. In control engineering maintaining the accuracy of the system is a best effort condition.

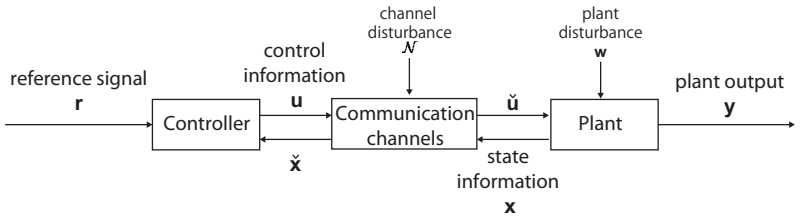

Figure 2.3 Feedback control system

In Fig. 2.4 for example, one of the outputs of the plant considered throughout this work, the rotary inverted pendulum, is shown. The figure shows the motion of the arm of the pendulum trying to follow a desired periodic motion from 0 to π radians in a 10 second cycle. The continuous curve represents the output when no disturbances (neither in the channel nor in the plant) are present in the system. Here, it can be seen that the motion is not perfectly rectangular and that there are slight overshoots and undershoots relative to the desired amplitude values. Regardless of this, the output value always settles after a certain amount of time, therefore the system is considered as stable. The dashed curve on the other hand, represents the case considering disturbances in the system. Here it can be seen how the overshoot and undershoot values are more pronounced and it also takes more time for the amplitude values to settle. This is an evidence that channel and plant disturbances can seriously worsen the stability of the system.

2.3 Feedback control system plant and controller

2.3.1 Rotary inverted pendulum

As a general example of a plant that requires continuous feedback control, in this system an underactuated object, the rotary inverted pendulum also known as the Furuta pendulum [11], is employed as the plant. The basic structure

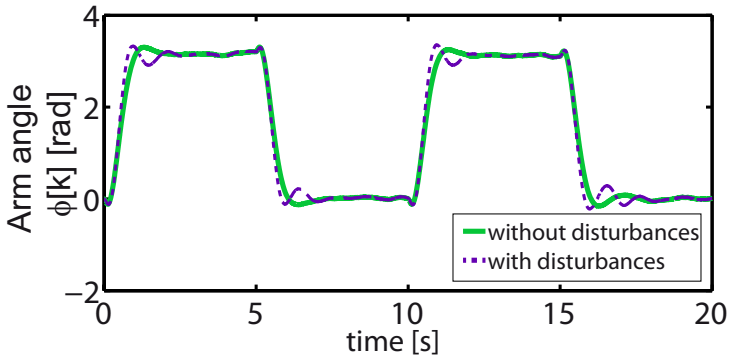

Figure 2.4 Example of the arm motion of the inverted rotary pendulum following a desired value without and with disturbance

of the rotary inverted pendulum is shown in Fig. 2.5. The outputs of the pendulum are considered to be the pendulum angle $\theta(t)$ and the arm angle of the pendulum $\phi(t)$ together with their respective derivatives (angular velocities). The pendulum angle $\theta(t)$ is defined as zero when the pendulum is in its upright position and as positive for counterclockwise rotation. The zero position for the arm angle $\phi(t)$ can be arbitrarily defined and the counterclockwise rotation has been defined as positive. The pendulum is controlled by applying a torque $u(t)$ on the rotating arm. The mass of the pendulum rod is defined as m_p, the length of the pendulum rod as L, the length of the rotating arm as r, and the moment of the arm as J_b. The moment of inertia of the pendulum rod is calculated as $J_p = m_p L^2/3$. Finally, g is the gravitational acceleration constant. The physical parameters considered for the rotary inverted pendulum throughout this work are shown in Table 2.1.

The dynamics of the pendulum are described by the following equations [8]:

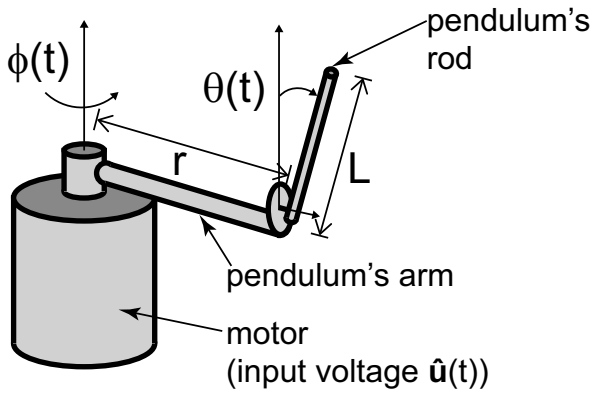

Figure 2.5 Basic structure of the rotary inverted pendulum

$$\begin{cases} a\ddot{\theta}(t) - a\dot{\phi}(t)^2 \sin\theta(t)\cos\theta(t) \\ \quad +c\ddot{\phi}(t)\cos\theta(t) - d\sin\theta(t) = 0 \\ c\ddot{\theta}(t)\cos\theta(t) - c\dot{\theta}(t)^2 \sin\theta(t) \\ \quad +2a\dot{\theta}(t)\dot{\phi}(t)\sin\theta(t)\cos\theta(t) \\ \quad\quad +(b + a\sin^2\theta(t))\ddot{\phi}(t) = u(t) \end{cases} \tag{2.3}$$

where

$$\begin{cases} a = J_p \\ b = J_b + m_p r^2 \\ c = m_p/(2rL) \\ d = Lgm/2 \end{cases} . \tag{2.4}$$

For the controller, a linear quadratic regulator (LQR) was chosen in this manuscript. In order to apply LQR techniques for the controller design, the system must first be linearized.

As the pendulum oscillates very close to the point of upward equilibrium, $\theta \approx 0$, therefore in the set of Eqs. (2.3), $\sin\theta \approx \theta$ and $\cos\theta \approx 1$. After applying these approximations, Eqs. (2.3) become linear as shown in the set

Table 2.1 Physical parameters for the considered inverted rotary pendulum.

Meaning	Symbol	Value
Mass of pendulum rod	m_p	0.016 kg
Length of pendulum rod	L	0.1 m
Length of rotary arm	r	0.2 m
Moment of inertia of the arm	J_b	0.0048 kgm^2
Motor direct-current resistance	R	8.3 Ω
Motor torque constant	K_m	0.023 Nm/A
Gear ratio	K_g	7.5
Gravitational acceleration	g	9.81 m/s^2

of Eqs. (2.5)

$$\begin{cases} a\ddot{\theta}(t) + c\ddot{\phi}(t) - d\dot{\theta}(t) = 0 \\ c\ddot{\theta}(t) + b\ddot{\phi}(t) = u(t) \end{cases} \tag{2.5}$$

then the state information $\mathbf{x}(t)$ is given by the following:

$$\mathbf{x}(t) = [\ \theta(t) \quad \dot{\theta}(t) \quad \phi(t) \quad \dot{\phi}(t)\ ]^T \tag{2.6}$$

where Eq. (6.1) can be expressed as:

$$\dot{\mathbf{x}}(t) = \mathbf{A}\mathbf{x}(t) + \mathbf{B}u(t) \tag{2.7}$$

where

$$\begin{aligned} \dot{\mathbf{x}}(t) &= \mathbf{A}\mathbf{x}(t) + \mathbf{B}u(t) \\ &= \begin{bmatrix} 0 & 1 & 0 & 0 \\ \frac{bd}{ab-c^2} & 0 & 0 & 0 \\ 0 & 0 & 0 & 1 \\ \frac{-cd}{ab-c^2} & 0 & 0 & 0 \end{bmatrix} \mathbf{x}(t) + \begin{bmatrix} 0 \\ \frac{-c}{ab-c^2} \\ 0 \\ \frac{a}{ab-c^2} \end{bmatrix} u(t). \end{aligned} \tag{2.8}$$

It must be noted that this research is based on linear approximations of the pendulum dynamics shown in Eqs. (2.5) and (2.8), and that the case where the pendulum falls from its upright position and must be raised again is not considered.

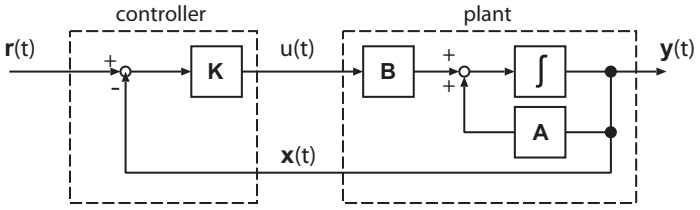

Figure 2.6 Continuous-time control system

2.3.2 Rotary inverted pendulum control scheme

In Fig. 2.6 the linearized model of the rotary inverted pendulum feedback contol system is shown. As inputs for the control system the reference values for each of the state quantities of the controlled object: $\Theta(t)$, $\dot{\Theta}(t)$, $\Phi(t)$, $\dot{\Phi}(t)$ are given. Then the reference signal or target value $\mathbf{r}(t)$ is represented by

$$\mathbf{r}(t) = [\ \Theta(t) \quad \dot{\Theta}(t) \quad \Phi(t) \quad \dot{\Phi}(t)\ ]^T. \tag{2.9}$$

The control input $\mathbf{u}(t)$ represents the pendulum's arm torque which is sent to the plant. Then control output $\mathbf{y}(t)$ is composed of the measured pendulum angle $\theta(t)$, the arm angle $\phi(t)$ and their respective variation values $\dot{\theta}(t)$ and $\dot{\phi}(t)$ which are fed back as the state information values in $\mathbf{x}(t)$ to the controller. The difference or deviation between the target value $\mathbf{r}(t)$ and the feedback state information values in $\mathbf{x}(t)$ is defined as $\mathbf{e}(t)$. The control input $\mathbf{u}(t)$ is then the inner product of the 1×4 feedback gain matrix $\mathbf{K}$ and the deviation $\mathbf{e}(t)$:

$$\mathbf{u}(t) = \mathbf{K}\mathbf{e}(t) = \mathbf{K}(\mathbf{r}(t) - \mathbf{x}(t)) \tag{2.10}$$

which is input into the plant.

2.3.3 Determination of the feedback gain

The feedback gain **K** is determined by applying a linear quadratic regulator (LQR). Here the calculated weights **Q** and **R** are shown as follows [8]:

$$\mathbf{Q} = \begin{bmatrix} 300 & 0 & 0 & 0 \\ 0 & 100 & 0 & 0 \\ 0 & 0 & 30 & 0 \\ 0 & 0 & 0 & 3 \end{bmatrix}, \ \mathbf{R} = [1000]. \tag{2.11}$$

Then the controller feedback gain is:

$$\mathbf{K} = \mathbf{R}^{-1}\mathbf{B}^{T}\mathbf{P} \tag{2.12}$$

where **P** is the positive definite solution of the Riccati equation:

$$\mathbf{A}^{T}\mathbf{P} + \mathbf{P}\mathbf{A} - \mathbf{P}\mathbf{B}\mathbf{R}^{-1}\mathbf{B}^{T}\mathbf{P} + \mathbf{Q} = 0. \tag{2.13}$$

2.4 Discretization of the control system

To be able to apply a digital control, the continuous-time control system must be discretized at sampling intervals of duration T_s.

2.4.1 System plant

The input signal for the discrete time control system is defined as $\mathbf{u}[k] = \mathbf{u}(kT_s)$. The input signal $\mathbf{u}[k]$ enters the controlled object as a zero-order hold continuous signal. From Eq.(2.8)

$$\mathbf{x}(t) = \exp(\mathbf{A}(t - t_0))\mathbf{x}(t_0) + \int_{t_0}^{t} \exp(\mathbf{A}(t - \tau))\mathbf{B}\mathbf{u}(\tau)d\tau \tag{2.14}$$

can be obtained substituting $t_0 = kT_s$, $t = (k + 1)T_s$ into this equation and considering that $\mathbf{u}(t)$ taken from $\mathbf{u}[k]$ is constant during the interval $kT_s \leq t <$

$(k+1)T_s$; we have a relationship between the controlling input $\mathbf{u}[k]$ and the state information $\mathbf{x}[k] = \mathbf{x}(kT_s)$, in discrete time as:

$$\begin{aligned} \mathbf{x}[k+1] &= \mathbf{A_d}\mathbf{x}[k] + \mathbf{B_d}\mathbf{u}[k] \\ &= \exp(\mathbf{A}T_s)\mathbf{x}[k] + \int_0^{T_s} \exp(\mathbf{A}\tau)d\tau \cdot \mathbf{B}\mathbf{u}[k] \end{aligned} \tag{2.15}$$

where $\mathbf{A_d}, \mathbf{B_d}$ are the discrete version of $\mathbf{A}$ and $\mathbf{B}$ respectively. Here, the exponential function matrix

$$\exp(\mathbf{A}T_s) = \sum_{i=0}^{\infty} \frac{\mathbf{A}^i {T_s}^i}{i!} \tag{2.16}$$

is defined.

2.4.2 Discrete time feedback control system

The discretized feedback control system is shown in Fig. 2.7. The expression for the discrete reference signal is given as follows:

$$\mathbf{r}[k] = \mathbf{r}(kT_s) = [\ \Theta[k] \quad \dot{\Theta}[k] \quad \Phi[k] \quad \dot{\Phi}[k]\ ]^T. \tag{2.17}$$

Then the state information and the control input take the following forms respectively: $\mathbf{x}[k] = \mathbf{x}(kT_s)$, $\mathbf{u}[k] = \mathbf{u}(kT_s)$. Similarly to Eq.(2.10) at the controller we have the deviation between the reference value and the feedback state information $\mathbf{e}[k]$, from which we obtain the discretized input control signal

$$\mathbf{u}[k] = \mathbf{K}\mathbf{e}[k] = \mathbf{K}(\mathbf{r}[k] - \mathbf{x}[k]). \tag{2.18}$$

2.4.3 Determination of the feedback gain at the controller

The discrete feedback gain is obtained in a similar manner to the continuous-time version of the feedback gain shown in Eqs. (2.12) and (2.13). In brief, the feedback gain $\mathbf{K}$ is

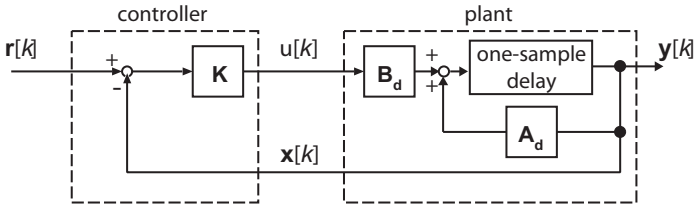

Figure 2.7 Discrete-time control system

$$\mathbf{K} = (\mathbf{B_d}^T \mathbf{P} \mathbf{B_d} + R)^{-1} (\mathbf{B_d}^T \mathbf{P} \mathbf{A_d}) \tag{2.19}$$

where $\mathbf{P}$ is the positive definite solution of the Riccati equation:

$$\mathbf{A_d}^T \mathbf{P} \mathbf{A_d} - \mathbf{P} - (\mathbf{A_d}^T \mathbf{P} \mathbf{B_d}^T)(\mathbf{B_d}^T \mathbf{P} \mathbf{B_d} + R)^{-1} (\mathbf{B_d}^T \mathbf{P} \mathbf{A_d}) + \mathbf{Q} = 0. \tag{2.20}$$

2.5 Summary

In this Chapter the main elements of the feedback control system being considered in this work, the controller and the plant, as well as their interactions were described. The way in which the controller verifies the condition of the plant to correct its behavior through its commands was shown.

Chapter 3

Power line environment

Power line communications has a long history as it has been in development since the early 1900's. The key advantage of PLC is the existence of electrical lines which are widely spread throughout the entire world. This can potentially save the costs of dedicated cabling and antennas and also serve as an alternative to reach areas in which wireless signals are blocked.

Nowadays it is a viable technology in both high and low data transmission speeds. Broadband power line communications has its use mainly as a last mile solution for internet distribution and indoor networking applications. However, its limitations for outdoor use, its short propagation range and possible interference with surrounding radio systems, present a great disadvantage when it comes to applications such as control of machines through the smart grid.

Narrowband power line communications, which is the main focus of this work, presents longer propagation distances due to the lower frequencies in use and less interference with existing radio systems. However, its low capacity prompts the use of more efficient communication techniques to take advantage of the limited bandwidth resource.

3.1 Power line communications versus wireless/wired

For the case of smart grid applications and the industry, power line communications is promising in the cases in which wireless cannot be used because of interference or obstacles that block the wireless signal. This can serve as a replacement or as a way to offer redundancy to wireless networks when very high reliability is required.

As shown in Fig. 3.1, wireless signals on the other hand can be blocked easily or interfered with, therefore reliability for industrial control applications and the smart grid is questionable. The main advantage of PLC over wireless and other dedicaded wired solutions is that PLC is already widely deployed and this existing infrastructure can overcome various obstacles. A very simple example is shown in Fig. 3.2. Another advantage of PLC is that as wireless, scalability can also be achieved as shown in Fig. 3.3. This is not the case for dedicated cabling, as the installation of new cabling may be required to achieve such a purpose.

Control and monitoring in the future grid requires low-delay, highly reliable communication between customers, local utilities and regional utilities. An essential element in this grid is the link between the customer sites and control centers opperated by a local utility. This communication must be bidirectional. To enable such a bidirectional communication, PLC, in special narrowband PLC (between 3 and 500 kHz), is attractive because of its possible use not only indoors but also outdoors [12]. Power line communications used in conjunction with other communication technologies to control machines for the smart grid can be seen in [13] and in [14] the existing power line infrastructure is used as an effective method of easily implementing a communication solution.

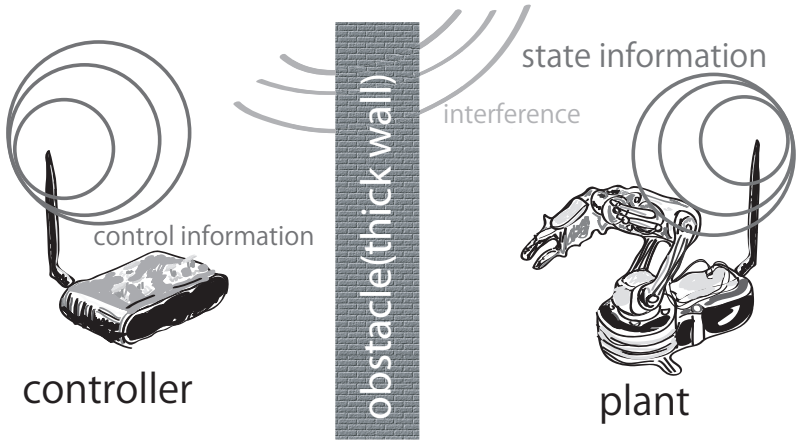

Figure 3.1 Wireless control and its issues

3.2 PLC: narrowband versus broadband

Broadband uses a wide frequency band, usually between 2 MHz and 30 MHz allowing for hundreds of Mbps of data rate. It is typically used for applications which require high speed such as high definition video, audio and the Internet.

Narrowband PLC systems, on the other hand, operate in the 3-500 kHz frequency range and include various frequency bands, namely the CENELEC, FCC, and ARIB frequency bands. It is used by electric utilities around the world for meter reading and load control and a few utility smart grid applications, and command-and-control applications for residence and industry use [15]. Narrowband PLC usually provides data rates which are just tens of kbps. Narrowband PLC is more suitable for applications which require low data rates such as command, control and monitoring. Besides this, narrowband PLC is suitable for its use outdoors because of its longer propagation distance and lower interference with other systems when compared to broadband PLC. This long distance range makes narrowband PLC an ideal candidate for con-

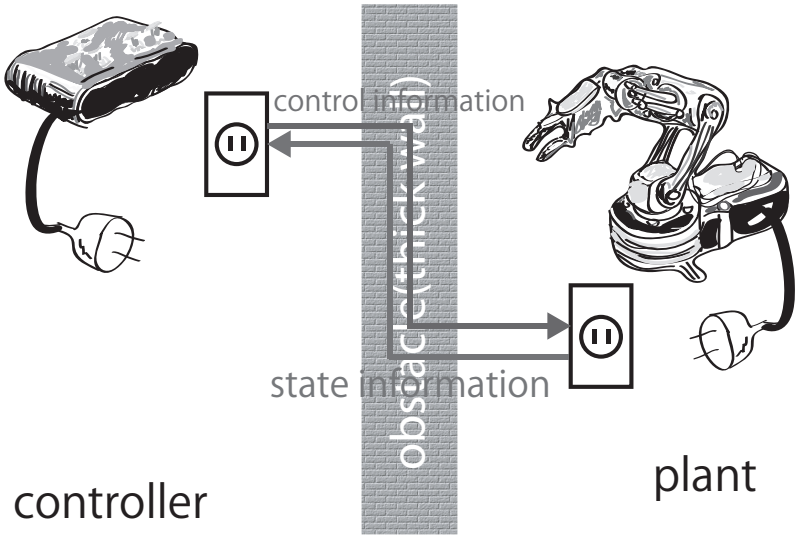

Figure 3.2 Simple scheme of a control system employing PLC

trol applications in the smart grid. Another advantage of narrowband PLC is the existence of multicarrier industry standards such as G3-PLC and PRIME which further extend the capability of the narrowband PLC medium [12].

A brief comparison of narrowband and broadband PLC can be seen in Table 3.1 taken from [16].

Regarding the modulation schemes employed for each case, broadband systems usually employ multi-carrier modulation schemes, whereas narrowband systems usually employ single-carrier modulation schemes.

Examples of single-carrier modulation schemes commonly used in narrowband PLC are On-Off Keying modulation, Binary Phase Shift Keying (BPSK), and Binary Frequency Shift Keying (BFSK). These provide reliable communication at a low power consumption and low cost. In this work, for the sake of simplicity, BPSK is applied.

There are also a few implementations of Spread Spectrum (SS) schemes,

and the recent application of multi-carrier modulation schemes to narrowband PLC, being Orthogonal Frequency Division Multiplexing (OFDM) the most popular one. Multi-carrier schemes present robustness against interference and frequency-selective distortions, however the narrowband frequencies greatly restrict the possible transmission rates.

3.3 Narrowband power line communications channel

In general, there are many channel characteristics which limit communication functionality through power lines, such as frequency-dependent attenuation, multipath distortion, and impulsive and background noise. However in a desire to take advantage of the infrastructure availability, limited communication through power lines has existed during many years [17].

Generic power line models are quite difficult to realize given the sudden changes in the networks caused by the connection and disconnection of various appliances. However, restraining the model to a finite time window, the channel can be has stationary characteristics and it can be modeled as a time-varying frequency-selective fading channel with various noise sources [17]. A more complete review on the power line model can be found in [18],[19].

Many electric devices connected to the power line network have a linear and time-invariant current-voltage relationship. However, some devices show a nonlinear behavior that provokes cyclic impedance properties with a period usually equal to half the AC mains cycle [20]. If the network is dominated by such devices, then the channel will exhibit a cyclic time-varying or in other words a cyclostationary behavior.

In recent studies it has been shown that the dominant components of noise in narrowband PLC are periodic and cyclostationary noise [21],[22]. It differs from additive white Gaussian noise which is commonly used in the modeling

of communication systems. There are many experimental results on PLC noise which have been reported on [23]. The types of noise in the power line can be summarized into three categories: background noise, periodic noise and asynchronous impulsive noise [12].

Background noise is generated by common residential and building electronic equipment. For frequencies less than 3 MHz usually the noise generated is nonwhite. For frequencies above 3 MHz, this noise is usually modeled as white Gaussian noise.

For frequencies below 3 MHz, which is the case including narrowband PLC, a low-frequency modulated sinusoid can be used to model narrowband noise.

In the case of impulsive noise, in order to understand the fundamental effects of this type of noise on PLC, its variations are modeled in a periodic fashion with amplitudes that are identical from pulse to pulse. In order to study the man-made impulsive noise environment, a model for its probability density function was expressed in [24]. However, this model does not define time-domain features [25].

Taking the above factors into consideration, the power line noise model developed in [25] is explained in the following section.

3.4 Power line noise model

In this work the main feature of narrowband power line communications being considered is its characteristic noise and attenuation. For narrowband (approximately 3 kHz to 500 kHz) PLC systems, dominant noise is bandlimited and its features are time variant and cyclic. These features vary synchronously with the AC mains voltage. For this type of narrowband PLC noise, a cyclostationary additive Gaussian noise with a zero mean and a variance synchronous to twice the frequency of the AC mains voltage is assumed [6],[25]. The instantaneous noise power is approximated through the use of the following

normalized function taken from [25]:

$$\hat{\sigma}^2(t) = \sum_{\ell=0}^{L-1} A_\ell |\sin(2\pi(t-\Delta)/T_{AC} + \theta_\ell)|^{n_\ell} \tag{3.1}$$

where T_{AC} is the period of the mains voltage for which the conventional value of $T_{AC} = 1/60$ s was assumed. An offset variable Δ has also been included here in Eq. (3.1) for the study of control signal timing in Chapter 4. This variable is considered to have a value of zero in the rest of the Chapters. In this model, a set of three parameters A_ℓ, θ_ℓ, and n_ℓ are considered. These parameters for $L = 3$ are shown in Table 3.2 and their derivation is explained in [25]. The instantaneous noise power function shown in Eq. (3.1) includes components of background noise, continuous periodic features of noise and periodic impulsive noise.

An example of a noise waveform generated using these parameters is shown in Fig. 3.4. The overlapped waveform represents the shape of the mains voltage. Additionally, two periods of the approximated instantaneous noise power or cyclostationary noise variance represented by Eq. (3.1) using the parameters in Table 3.2 are shown in Fig. 3.5. To show the contrast, a sample of a noise waveform with a constant variance has been included in Fig. 3.6.

3.5 Packet error rate

In the control system considered in this work, as a simplification, noise power is assumed to be invariant throughout the duration of a packet. For simplicity, the binary phase shift keying (BPSK) modulation scheme was chosen. The probability of bit error (BER) for the BPSK modulated signal with a packet index n and a packet period T_p is the following:

$$P_b[n] = \frac{1}{2}\left(1 - \text{erf}\left(\sqrt{\frac{\gamma}{\hat{\sigma}^2(nT_p)}}\right)\right), \tag{3.2}$$

where γ is the average signal-to-noise ratio per bit. If the packet length in bits is given as ℓ_p, the packet loss rate (PER) is:

$$P_e[n] = 1 - (1 - P_b[n])^{\ell_p} . \tag{3.3}$$

Fig. 3.7 shows examples of the packet error rate for the cyclostationary noise and the stationary noise cases and how it varies depending on the average signal-to-noise ratio per bit. The stationary noise is white Gaussian noise with a variance that is not time variant. In Figs. 3.8 and 3.9 the average packet error rate curves plotted against the average signal-to-noise ratio are shown for both the cyclostationary and stationary noise cases. In these graphs it can be seen that for low SNR conditions, cyclostationary noise offers a better PER and BER than stationary noise. This is due to the fact that at low SNR conditions in the cyclostationary noise case, the periods of low noise dominate the performance. In the case of stationary noise there are no periods of low noise present so the performance is worse. Under high SNR conditions, the cyclostationary noise case shows a worse performance and this is due to the fact that the peaks and periods of high noise dominate the performance. Under high SNR conditions for the stationary case, the steady level of noise is easily overcome with better signal power.

3.6 Summary

In this chapter the main features of the power line being considered in this study were explained. Broadband as opposed to narrowband power line communications has a few disadvantages in outdoor use for control, specially if the distances between the contoller and plant are considerable. Additionally, the prevalent cyclostationary feature of noise and attenuation in the power lines with its somewhat deterministic nature, presents itself as a feature that may be exploited to improve the performance of control applications. This will be explained in more depth in Chapters 4, 5 and 6.

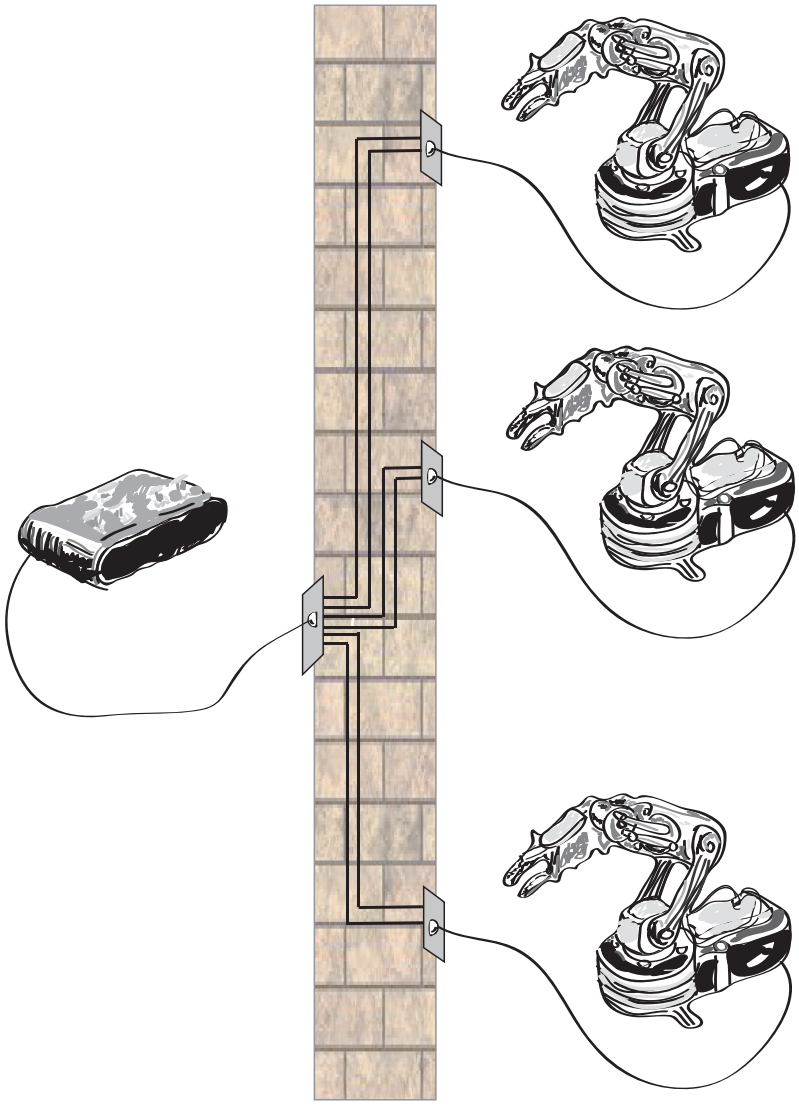

Figure 3.3 Multiple machine control system employing PLC

Table 3.1 Comparison of Narrowband and Broadband PLC.

	Narrowband PLC	Broadband PLC
Frequency	Up to 500 kHz	Over 2 MHz
Data rate	Up to 200 kbps	Over 1 Mbps
Modulation	FSK,S-PSK,BPSK,SS,OFDM	OFDM
Applications	Building Automation Renewable Energy Advanced Metering Street Lighting Electric Vehicle Smart Grid	Internet HDTV Audio Gaming
Standards	G3-PLC PRIME	IEEE 1901 HomePlug AV
Providers	Ariane Controls Cypress Echelon Maxim ST Microelectronics Texas Instruments Yitran	Atheros Broadcom Lantiq Marvell Maxim Sigma

Table 3.2 Parameters for the narrowband PLC noise model.

ℓ	A_ℓ	θ_ℓ[deg]	n_ℓ
0	0.230	0	0
1	1.38	−6	1.91
2	7.17	−35	1.57×10^5

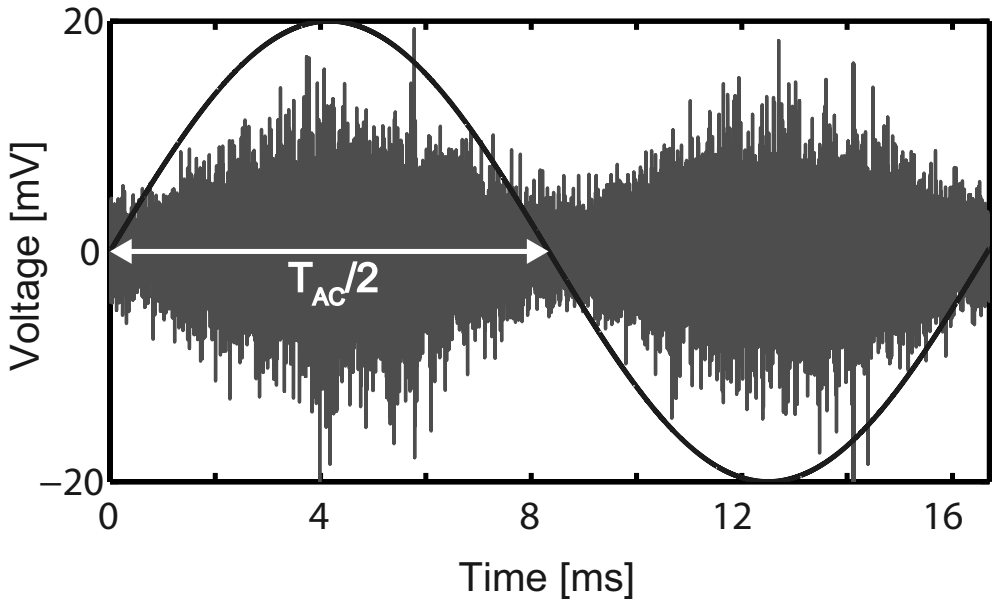

Figure 3.4 Example of computer generated power line noise (normalized) and overlapped mains voltage waveform (amplitude scaled).

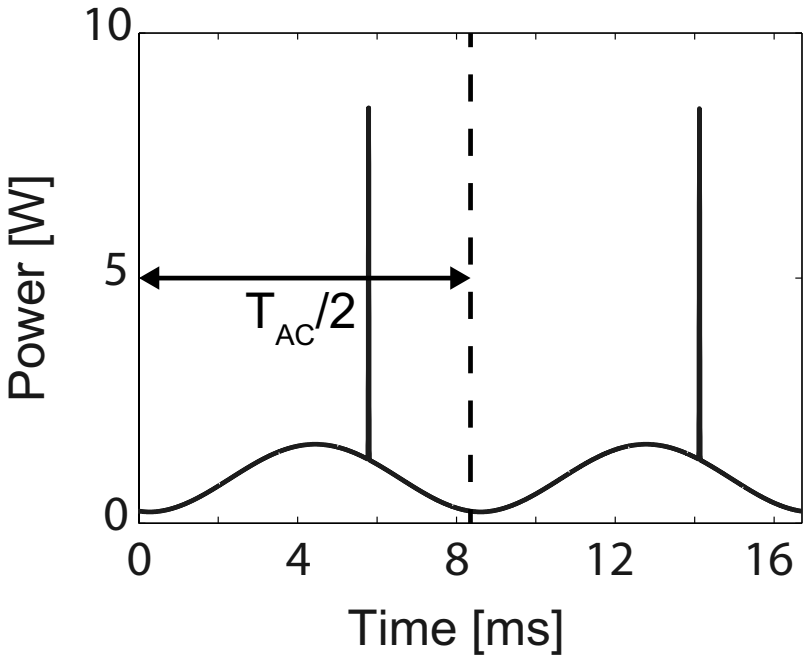

Figure 3.5 Example of approximated cyclostationary noise variance.

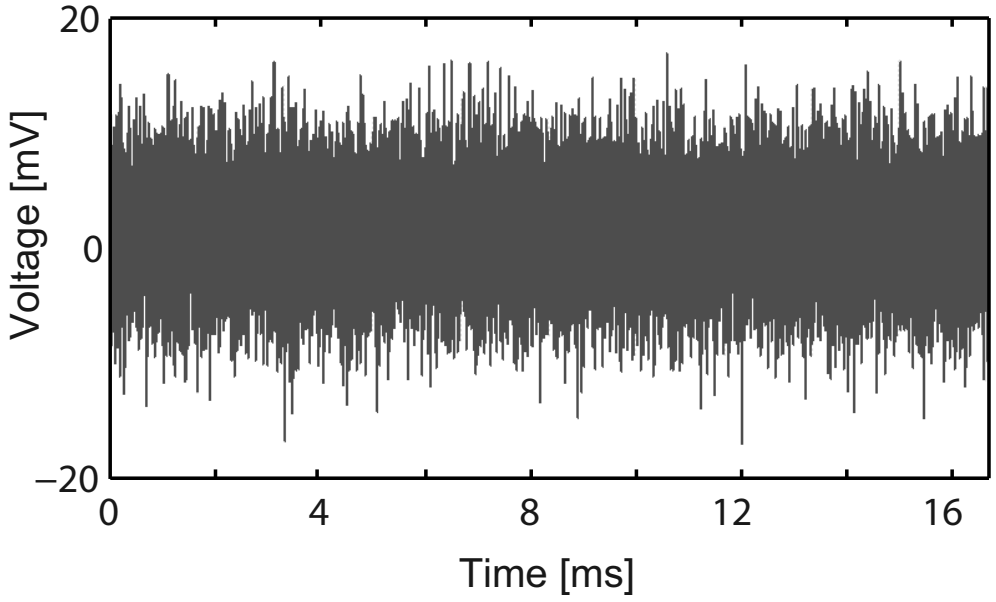

Figure 3.6 Example of computer generated stationary noise.

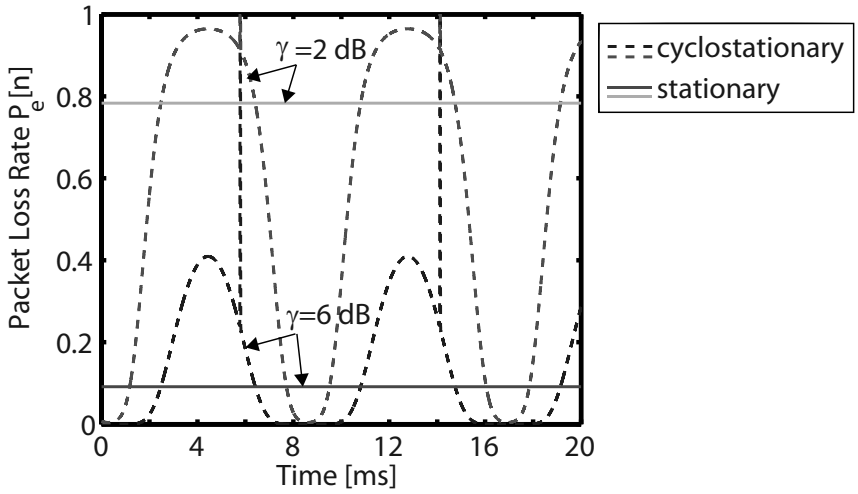

Figure 3.7 Packet loss rate comparison for the cyclostationary and stationary noise cases.

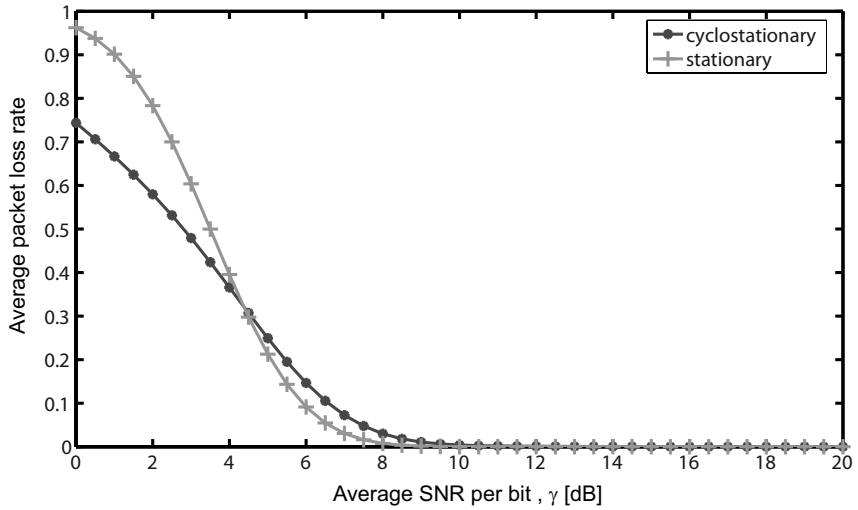

Figure 3.8 Average packet loss rate vs. average SNR for the cyclostationary and stationary noise cases (linear scale)

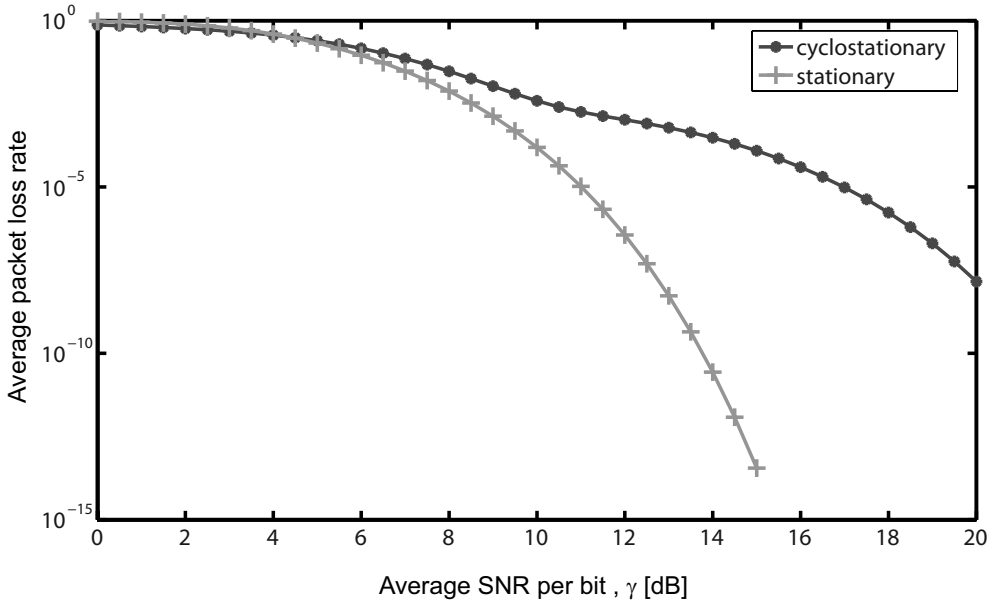

Figure 3.9 Average packet loss rate vs. average SNR for the cyclostationary and stationary noise cases (semilogarithmic scale)

Chapter 4

Machine control through power line communications[38],[39],[40]

It was mentioned in the previous chapters that power lines serve as excellent candidates for control applications due to their wide availability and potential in the realization of the future smart grid. There is also a potential for application in industrial environments where cost and resources must be saved.

As in any communication medium, communication errors may occur in power lines. This is mainly due to the presence of noise of various kinds and interference from sources external to the power lines. To deal with such an environment and be able to carry out control, a method to transfer the commands to the plant and the responses from the plant, must be devised. In this chapter the interactions between the various control signals, the rate at which they are transferred and the noise in the channel are studied. This is done by comparing a system whose communication channel is affected solely by stationary noise against another one affected by cyclostationary noise.

4.1 Control system under packet loss environment

Inside the discrete-time feedback control system, the control information is sent from the controller to the plant, and the state information measured on the plant side is then sent to the controller through a power line feedback loop.

This power line feedback loop between the controller and the plant is shown in Fig. 4.1. This feedback loop includes the transmitters and receivers on both ends. Also it is important to mention that in this Chapter the purpose is to analyze how the disturbances in the channel affect the performance of the control, therefore disturbances in the plant **w** shown in Fig. 2.3, are not considered in this Chapter.

For the system in Fig. 4.1, two poweline channels are required, one for the discrete control information $\mathbf{u}[k]$ that is sent from the controller to the plant and the other for the discrete state information $\mathbf{x}[k]$ that is fed back from the plant to the controller.

Fig. 4.1 shows the considered PLC control system. The digital system sampling rate is $1/T_s$ with a sampling index k and the packet rate at which information packets are sent through the channels is $R_p = 1/T_p = 1/NT_s$, where N is a positive integer and T_p is the packet period. In Fig. 4.1 the transmitted control information has been labeled as $\mathbf{u}_t[n]$ and the received control information $\mathbf{u}_r[n]$. Similarly, the transmitted state information is $\mathbf{x}_t[n]$ and the received state information is $\mathbf{x}_r[n]$. The relationship between the transmitted information and $\mathbf{u}[k]$ and $\mathbf{x}[k]$ is shown as follows:

$$\mathbf{u}_t[n] = u[Nn]$$

$$\mathbf{x}_t[n] = \mathbf{x}[Nn]$$

where the packet index is:

$$n = 0, 1, 2, \cdots \tag{4.1}$$

If there are no errors in the PLC channel, the received control information is $\mathbf{u}_r[n] = \mathbf{u}_t[n]$ and the received state information is $\mathbf{x}_r[n] = \mathbf{x}_t[n]$. Since packets are sent at constant intervals, it can be known through a simple mechanism (a packet sequence number for example) if packet losses have occurred. In this system perfect error detection is assumed and one-bit errors in packets are counted as packet losses. In other words, if an error occurs in a packet, the whole packet becomes discarded. On the plant side, the received control information $\mathbf{u}_r[n]$ is used as the estimated value for $\mathbf{u}[k]$. If a packet loss occurs, the plant reuses the last value. In the plant, the estimated control signal $\hat{\mathbf{u}}[k]$ is represented as follows:

$$\hat{\mathbf{u}}[k] = \begin{cases} \mathbf{u}_r[\lfloor k/N \rfloor] & \text{if no packet losses occur} \\ \hat{\mathbf{u}}[k-1] & \text{otherwise} \end{cases} . \tag{4.2}$$

This estimated signal $\hat{u}[k]$ is input into the plant and the state information $\mathbf{x}[k]$ is sent back as packets to the controller and is received as an estimated state information signal $\hat{\mathbf{x}}[k]$. Similarly in the controller the estimated state information signal $\hat{\mathbf{x}}[k]$ is given as

$$\hat{\mathbf{x}}[k] = \begin{cases} \mathbf{x}_r[\lfloor k/N \rfloor] & \text{if no packet losses occur} \\ \hat{\mathbf{x}}[k-1] & \text{otherwise} \end{cases} . \tag{4.3}$$

Figs. 4.2 and 4.3 show examples of how the control information packets are transferred through the channel. Fig. 4.2 shows the case when no errors occur in the channel. Fig. 4.3 shows the case in which errors occur and packets are discarded. The transfer of state information through the channel is treated in a similar fashion.

The packet loss rate depends on the power line channel noise. The noise in a power line channel is assumed to be cyclostationary. Each packet is independently lost with a time-varying probability $P_e[n]$. The noise model considered for the power line channel is explained to a further extent in Chapter 3.

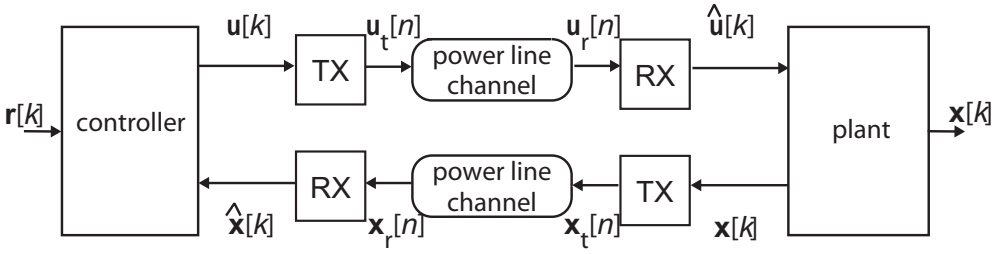

Figure 4.1 Block diagram of a power line control system

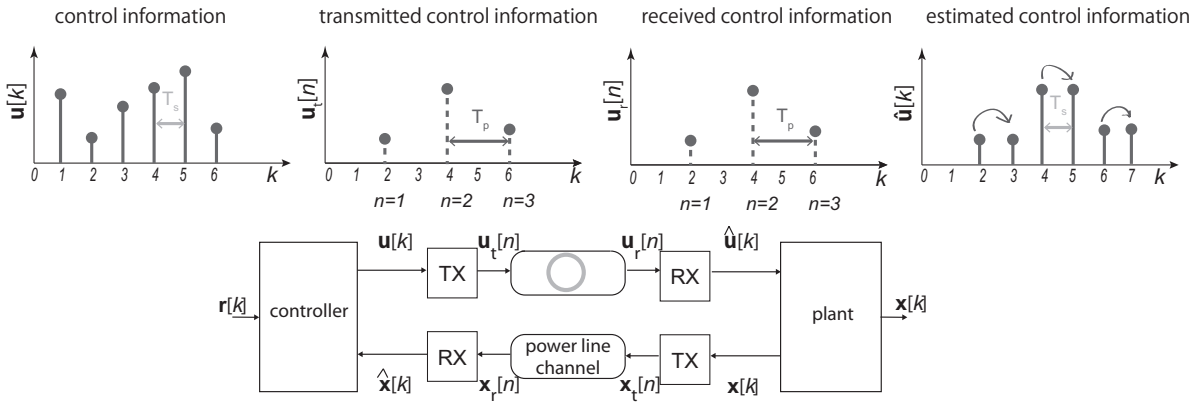

Figure 4.2 Example of the transfer of control information signals through the power line channel with no errors

4.2 Simulation model

This section discusses the influence of the packet loss rate on the control of the inverted rotary pendulum in both stationary and cyclostationary noise channel environments. The rotary pendulum is controlled to make its arm angle $\phi[k]$ follow the target value $\Phi[k]$, while keeping the pendulum in an upright position, or in other words trying to maintain $\theta[k] = 0$. This means that the reference signal $\mathbf{r}[k]$ will have the following form:

$$\mathbf{r}[k] = [0\ 0\ \Phi[k]\ 0]^{\mathrm{T}}. \tag{4.4}$$

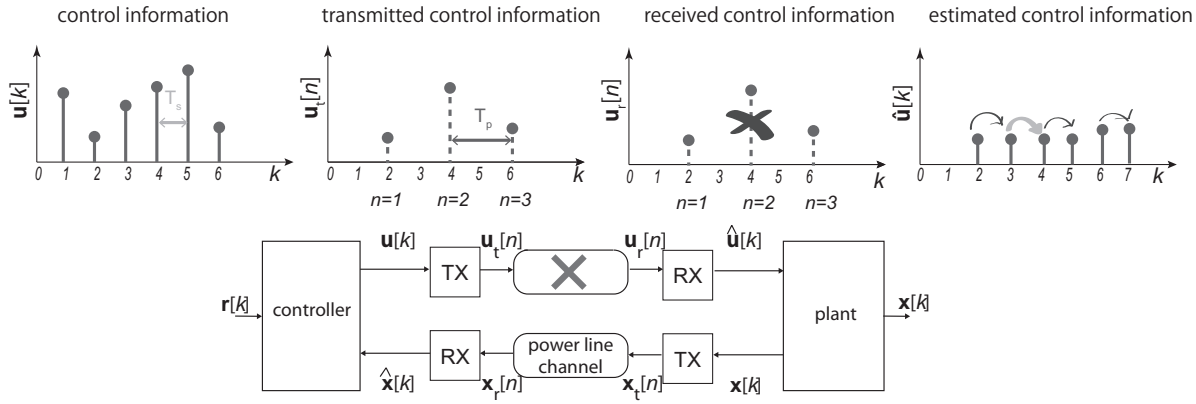

Figure 4.3 Example of the transfer of control information signals through the power line channel with errors

The simulation runs start from the initial state $\mathbf{x}[0] = [10^{-6}\ 0\ 0\ 0]^{\mathrm{T}}$. For simulation purposes $\theta[0]$ has been arbitrarily set to 10^{-6} rad which is a value very close to zero. The pendulum is considered to fall down in the range $|\theta[k]| > \frac{\pi}{6}$ and once this happens, the simulation run is terminated. The digital system sampling rate is set to $1/T_s = 1024$ Hz and the packet error probability is time varying in the cyclostationary case and fixed in the stationary case for given signal-to-noise ratio values, as shown in Fig. 3.7. The target value of the arm angle $\Phi[k]$ is a rectangular wave,

$$\Phi[k] = \begin{cases} \pi & iT \le kT_s < (i + \frac{1}{2})T \\ 0 & (i + \frac{1}{2})T \le kT_s < (i + 1)T \end{cases} \tag{4.5}$$

where $i = 0, 1, 2...$ and $T = 10$ s. The simulation parameters are summarized in Table 4.1. The gain $\mathbf{K}$ is calculated according to the different packet rates R_p using the following values for the weights $\mathbf{Q}$ and $\mathbf{R}$ taken from [8].

$$\mathbf{Q} = \begin{bmatrix} 300 & 0 & 0 & 0 \\ 0 & 100 & 0 & 0 \\ 0 & 0 & 30 & 0 \\ 0 & 0 & 0 & 3 \end{bmatrix}, \ \mathbf{R} = [1000]. \tag{4.6}$$

Table 4.1 Simulation parameters.

Meaning	Value
Modulation scheme	BPSK
Packet length	40 bits
Digital sampling rate	1024 Hz
Frequency of AC signal	60 Hz
Pendulum angle target value	0 rad
Arm's period of motion	10 s
Arm angle target values	0 to π rad

To simulate the random starting time for the transfer of the control signals, the variable Δ in Eq. (3.1) takes random values between 0 and $T_{AC}/2$. This prevents the noise cycle from being intentionally synchronized to the transfer of signals during the simulation.

4.3 Numerical examples

Figs. 4.4 and 4.5 show the input and output signals for the plant in the cyclostationary noise channel and in a stationary noise channel respectively for one simulation trial. In both cases the same SNR $\gamma = 4$ dB and the same packet rate $R_p = 128$ packets/s are considered. It can be seen that for the cyclostationary noise channel case, the pendulum keeps itself stable and the arm follows the motion of the reference signal throughout the duration of the trial. However, in the stationary noise channel case it is noted that for the same average signal-to-noise ratio and packet rate values, the pendulum falls after 10 seconds.

For Figs. 4.6 and 4.7 simulation runs of 100 s for the cyclostationary and the stationary noise channels are executed 5000 consecutive times and the respective pendulum fall rates are calculated. Fig. 4.6 shows the results for

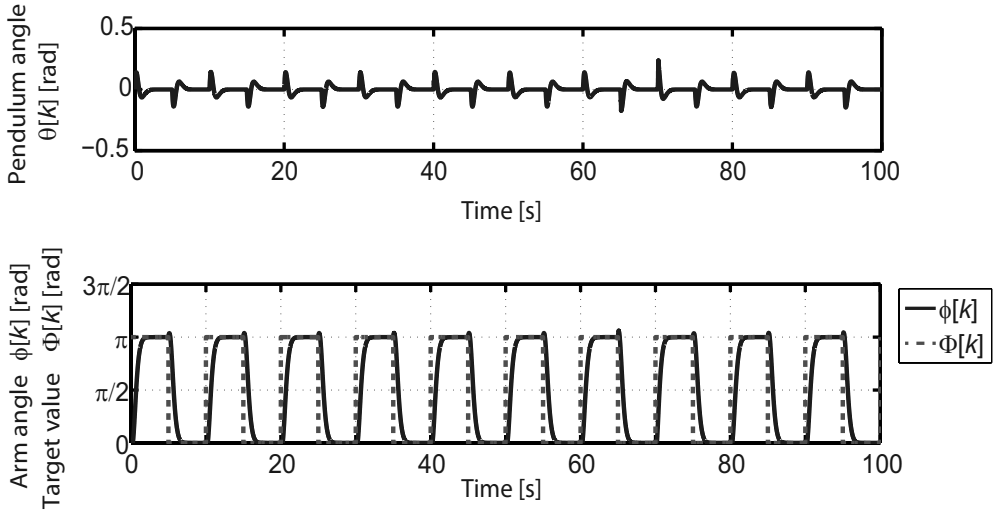

Figure 4.4 Example of pendulum angle $\theta[k]$ and arm angle $\phi[k]$ outputs and the input reference signal $\Phi[k]$ in a cyclostationary noise channel with $\gamma = 4$ dB and $R_p = 128$ packets/s.

three average signal-to-noise ratio values that are individually tested while the packet rate varies. Fig. 4.7 shows the results for three packet rate values that are individually tested while the average signal-to-noise ratio varies from 0 dB to 6 dB.

In Fig. 4.6 it can be seen that in the cyclostationary noise channel case for example, when $\gamma = 0$ dB, the pendulum stops falling at $R_p = 1024$ packets/s. However, in the stationary noise channel case, the pendulum falls regardless of how high the packet rate may be. It is clearly demonstrated that the performance in the cyclostationary noise channel is better as the pendulum presents lower fall rates in all cases. The reason for this is that the plant used in this system has a response that is relatively slow compared to the noise power variations in the power line case. This is proved by the fact that even with a slow data rate such as 8 packets/s, the pendulum can still be kept under better control in the cyclostationary case. These cyclic power variations are not present in the stationary noise case, therefore if the noise conditions are high, control

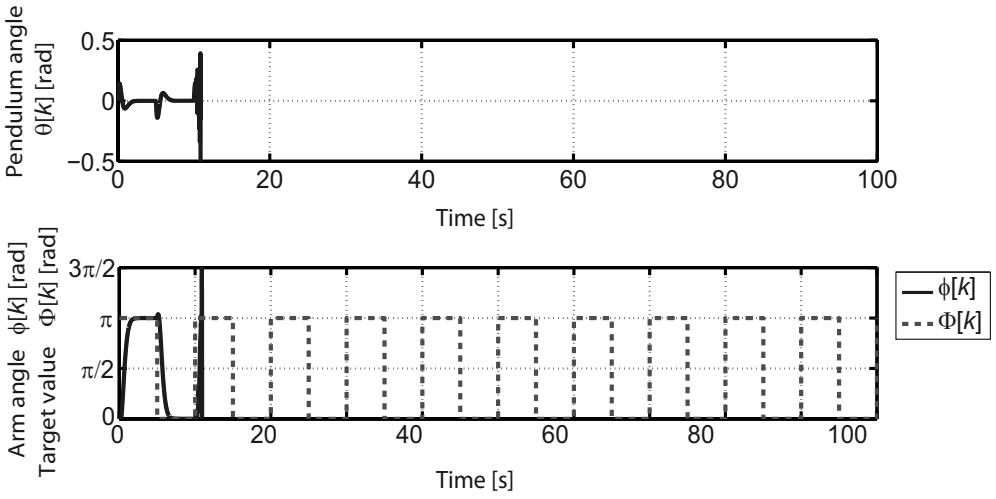

Figure 4.5 Example of pendulum angle $\theta[k]$ and arm angle $\phi[k]$ outputs and the input reference signal $\Phi[k]$ in a stationary noise channel with $\gamma = 4$ dB and $R_p = 128$ packets/s.

signals simply cannot go across the channel and this is a steady condition.

In Fig. 4.7 improvements can be seen for the three different values of R_p as γ is increased in the cyclostationary noise channel case. For example, for the $R_p = 32$ packets/s curve, the fall rate starts dropping at $\gamma = 2$ dB for the cyclostationary noise channel case, whereas it starts dropping at $\gamma = 3$ dB in the stationary noise channel case.

To confirm and summarize what has been found up to this point, in Fig. 4.8 it can be seen what occurs if the offset variable Δ in Eq. (3.1) is varied from 0 to $\Delta_t = T_{AC}/2$. The tests were carried out for a packet rate $R_p = 8$ packets/s and average signal-to-noise ratio conditions of 0, 2, and 4 dB. When the offset is $0.5\Delta_t$ the performance is worst for every γ. The reason for this is that at this value of Δ the information is sent exactly at the middle of the noise power cycle, when the noise and therefore the packet loss rate is highest. On the other hand the performance improves when the offset is close to 0 or close to Δ_t. At these two values of Δ noise is at its lowest levels since these values

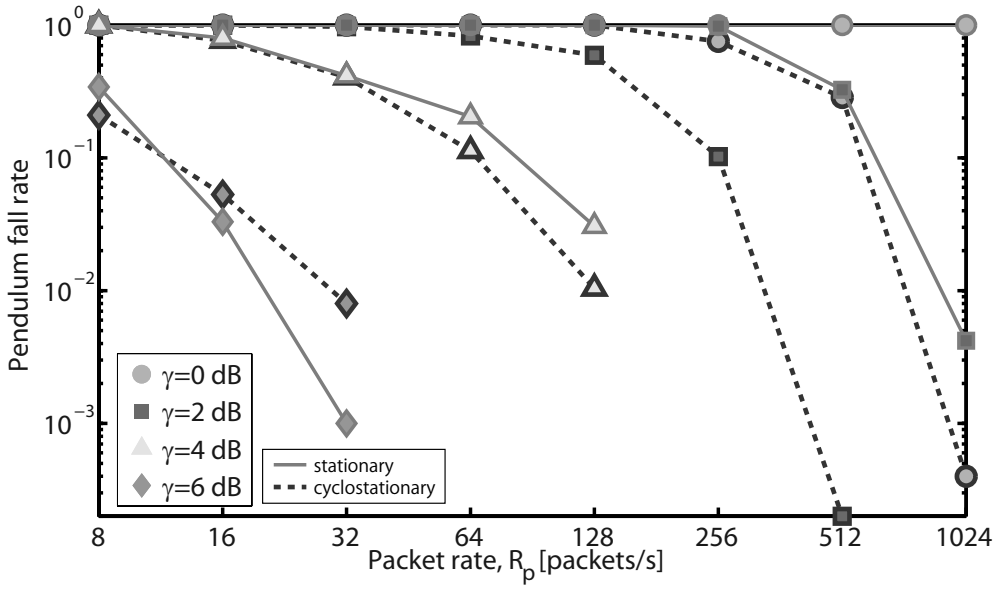

Figure 4.6 Pendulum fall rate for stationary and cyclostationary noise channels with varying packet rates.

mark the beginning and end of the noise power cycle. These two facts confirm that there are times at which the signals can be sent with little errors and times at which it is practically impossible to successfully transmit the signals, and such behavior is periodic.

To investigate what happens under conditions in which $\gamma > 4$ dB the corresponding tests were performed and included in Figs. 4.9 and 4.10. In these figures it can be observed that, when γ is approximately above 5 dB, the behavior under stationary noise conditions begins to improve at a higher rate than the behavior under cyclostationary noise conditions. This is also evident in Fig. 4.6 as a sudden flip in the behavior of the curves can be seen for the case in which $\gamma = 6$ dB, and in Fig. 4.7 it can be observed for all curves for values approximately above 4.5 dB. This is due to the fact that for higher signal-to-noise ratio values (lower pendulum fall rates), the impulsive components and high noise instants of the cyclostationary noise dominate the behavior. On the

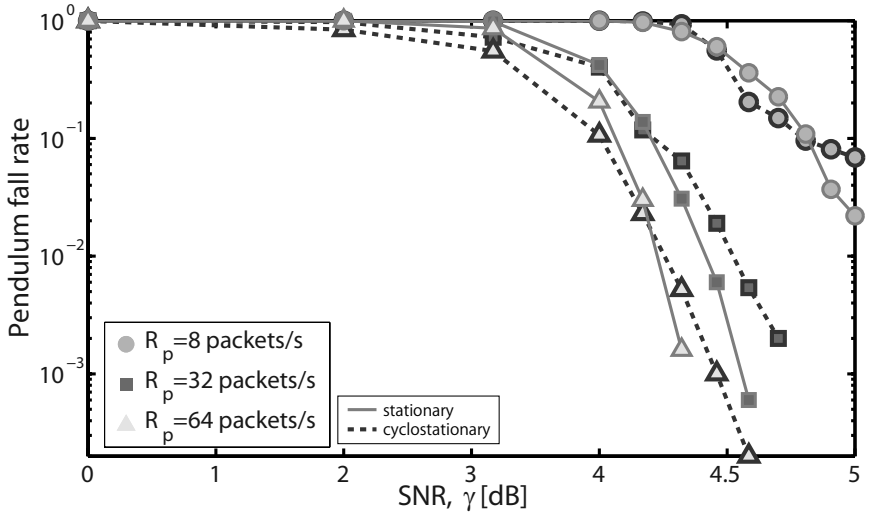

Figure 4.7 Pendulum fall rate for stationary and cyclostationary noise channels with varying average SNRs per bit.

other hand, for values lower than 5 dB, the instants of low noise dominate the behavior.

4.4 Summary

In this chapter shows the way in which control signals are transferred through the feedback control system considered in this work. The various interactions between the transfer rate of signals and the type and level of noise affecting the signals was studied. It was observed that in effect, the cyclostationary noise environment presents an advantageous situation for the case in which SNR is relatively low. This is an advantage that may be exploited to improve control performance in a system that uses PLC. In the following two chapters this will be further explored.

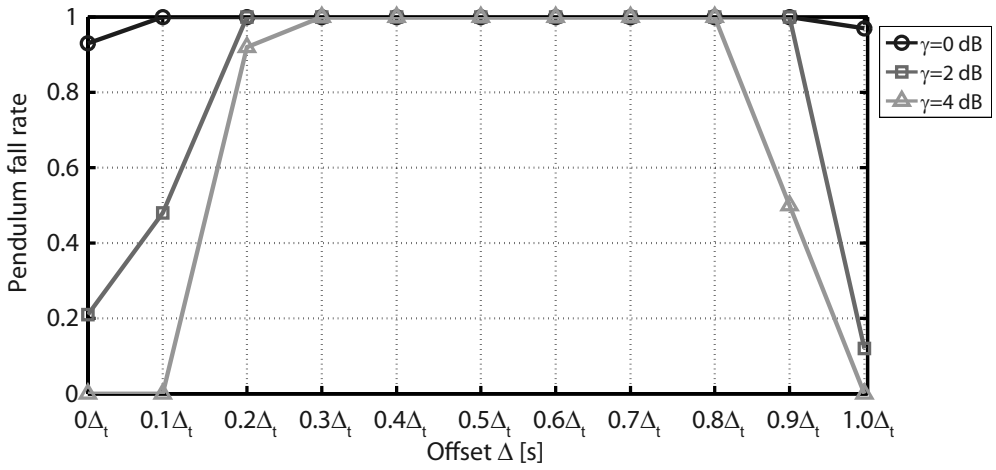

Figure 4.8 Pendulum fall rate for a cyclostationary noise channel with a fixed packet rate $R_p = 8$ packets/s and a varying control signal transfer start offset Δ ($\Delta_t = T_{AC}/2$).

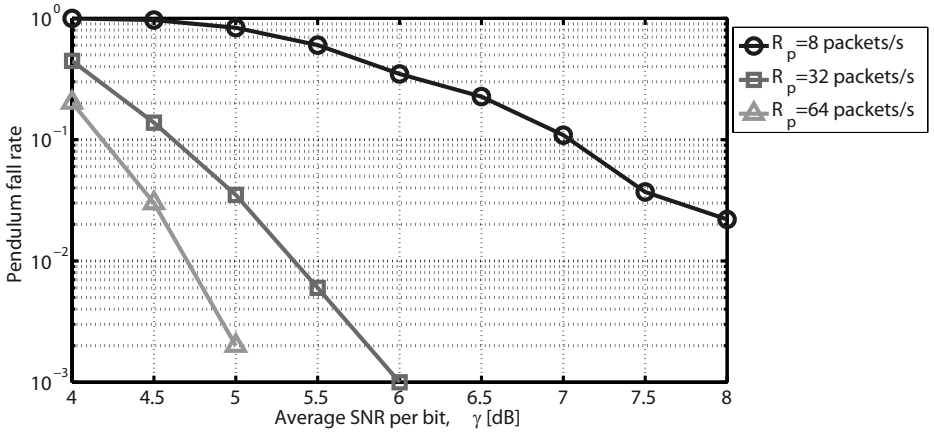

Figure 4.9 Pendulum fall rate for stationary noise channel with varying average SNRs per bit (1000 trials of 100 seconds each).

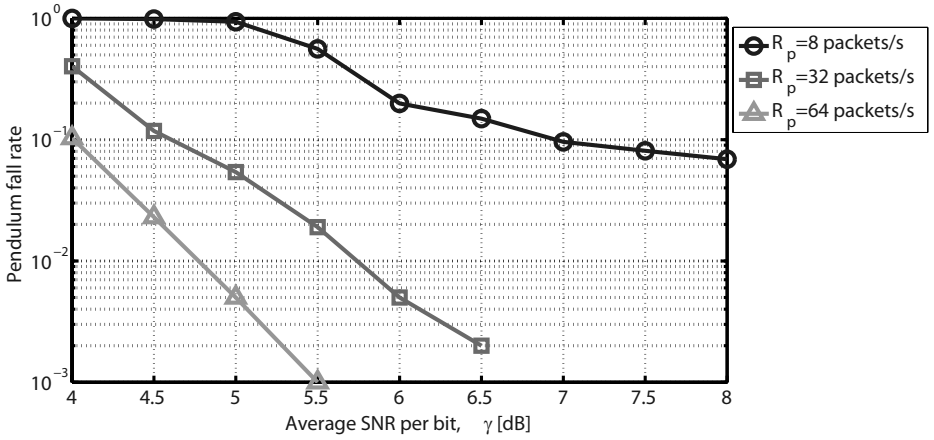

Figure 4.10 Pendulum fall rate for cyclostationary noise channel with varying average SNRs per bit (1000 trials of 100 seconds each).

Chapter 5

Improvement of single machine control using narrowband PLC[41],[42],[43]

In PLC the attenuation and noise both present cyclostationary features that may be exploited to improve the control for a single machine. In this section a predictive control method is applied to achieve this purpose. Taking advantage of the low noise instants additional predicted information is sent to the plant for use when the high levels of noise cause loss of information. In an ideal situation, the presence of disturbance in the plant is disregarded and the predicted commands can have a very high accuracy (not perfect if the errors in the channel are still being considered). However the accuracy of predictive control is limited by the presence of disturbance in the plant and this is also shown in this chapter.

5.1 Feedback Control System

Fig. 5.1 shows a general layout of a discrete-time feedback control system with power line channels as its feedback loop. In the system, the discrete-time control information $\mathbf{u}[k]$ is sent from the controller to the plant and the

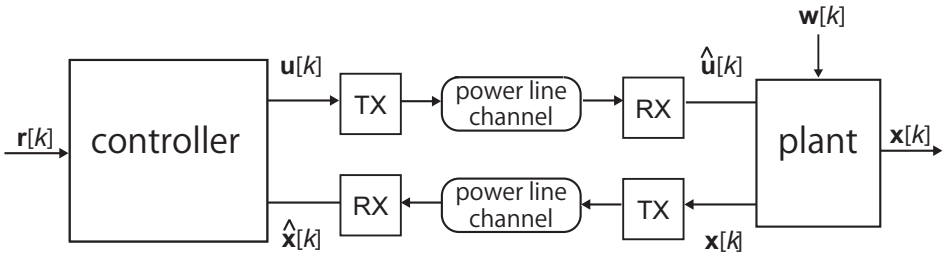

Figure 5.1 Block diagram of a discrete control system with a power line as a feedback loop.

discrete-time state information $\mathbf{x}[k]$ is fed back from the plant to the controller (both in form of packets). The packets are sent every T_s at time $t = kT_s$ and the sampling index k is a non-negative integer. In Fig. 5.1, TX denotes a transmitter and RX is a receiver. If there are no errors in the PLC channel, the output of RX on the plant side $\hat{\mathbf{u}}[k]$ is identical to $\mathbf{u}[k]$ and the output of RX on the controller side $\hat{\mathbf{x}}[k]$ is $\mathbf{x}[k]$. If there is at least a one-bit error in a packet, RX discards the packet and estimates substitutional information as described in section 5.3. The vector $\mathbf{w}[k]$ represents the plant disturbance. Such a disturbance is thought to be a mechanical vibration, friction in the actuator, and inaccuracy of the sensors for example.

As an example of the plant, a rotary inverted pendulum is employed. The basic structure of the rotary inverted pendulum with continuous-time inputs and outputs is shown in Fig. 2.5. The pendulum's rod mass is defined as m_p, and the rod's length is defined as L. The pendulum's arm length is r and the arm's central moment of inertia is defined as J_b. In Fig. 2.5, $\theta(t)$ is defined as the pendulum angle and $\phi(t)$ is defined as the arm angle. The objective of the control is to make $\theta(t)$ and $\phi(t)$ follow the reference vector function $\mathbf{r}(t)$. In order to achieve this objective, the controller calculates the necessary input value, or the voltage to the motor $\mathbf{u}(t)$.

5.2 Power line channel considerations

In general, PLC channels present cyclic features in both the noise and the attenuation, which are synchronous to the AC mains voltage [6],[25]. Therefore PLC shows a cyclic variation of its bit error rate (BER) and consequently of its packet error rate (PER). For simplicity, the noise is assumed to be the dominant factor for the cyclic features of communication quality and that its SNR is $1/\hat{\sigma}^2(t)$ where $\hat{\sigma}^2(t)$ is the noise power as a time function. The SNR is also assumed to be constant throughout the duration of each packet. Under the above assumption the model presented in Chapter 3 for the PER is derived and is described in Eq. (5.1) where the BER is Eq. (5.2) and the noise power is Eq. (5.3) based on the noise model of [25]. In this case notice that the packet index n has been replaced by the sampling index k and the packet perdiod T_p was replaced by the sampling period T_s. It is also worth mentioning that Δ from here on is considered to be zero so it has been eliminated in Eq. (5.3).

$$P_e[k] = 1 - (1 - P_b[k])^{\ell_p} \tag{5.1}$$

$$P_b[k] = \frac{1}{2}\left(1 - \operatorname{erf}\left(\sqrt{\frac{\gamma}{\hat{\sigma}^2(kT_s)}}\right)\right) \tag{5.2}$$

$$\hat{\sigma}^2(t) = \sum_{\ell=0}^{L-1} A_\ell |\sin(2\pi t/T_{AC} + \theta_\ell)|^{n_\ell}. \tag{5.3}$$

T_{AC} is the period of the mains voltage, and its value is 1/60 s.

5.3 Feedback Control without and with Predictive Control

5.3.1 Conventional Feedback Control without predictive control

The algorithms for the conventional method are summarized as follows. At the plant side, the estimated control signal $\hat{\mathbf{u}}[k]$ is represented as:

$$\hat{\mathbf{u}}[k] = \begin{cases} \mathbf{u}[k] & \text{no packet loss} \\ \mathbf{0} & \text{otherwise} \end{cases} . \tag{5.4}$$

This estimated signal $\hat{\mathbf{u}}[k]$ is input to the plant and at the next transmission instant $t = (k + 1)T_s$, the state information $\mathbf{x}[k + 1]$ is sent back as packets to the controller and is received as an estimated state information signal $\hat{\mathbf{x}}[k + 1]$. At the controller side the estimated state information signal $\hat{\mathbf{x}}[k + 1]$ is given by:

$$\hat{\mathbf{x}}[k+1] = \begin{cases} \mathbf{x}[k+1] & \text{no packet loss} \\ \mathbf{A_d}\hat{\mathbf{x}}[k] + \mathbf{B_d}\mathbf{u}[k] & \text{otherwise} \end{cases} . \tag{5.5}$$

Details on the vectors $\mathbf{A_d}$ and $\mathbf{B_d}$ are shown in chapter 2.

In Fig. 5.2 a simple case in which the signals are sent only during instants of low noise at a packet rate $R_p = 1/T_s = 120$ packets/s is shown. Fig. 5.3 illustrates the case in which the packet rate is doubled to $R_p = 240$ packets/s. In Fig. 5.3 the transmission of packets during both high and low noise instants can be observed. These packet rate values have been deliberately chosen to match the cyclic features of noise. In this model packet transmission delays are not considered, therefore the arrows that represent packet transmissions are perfectly vertical.

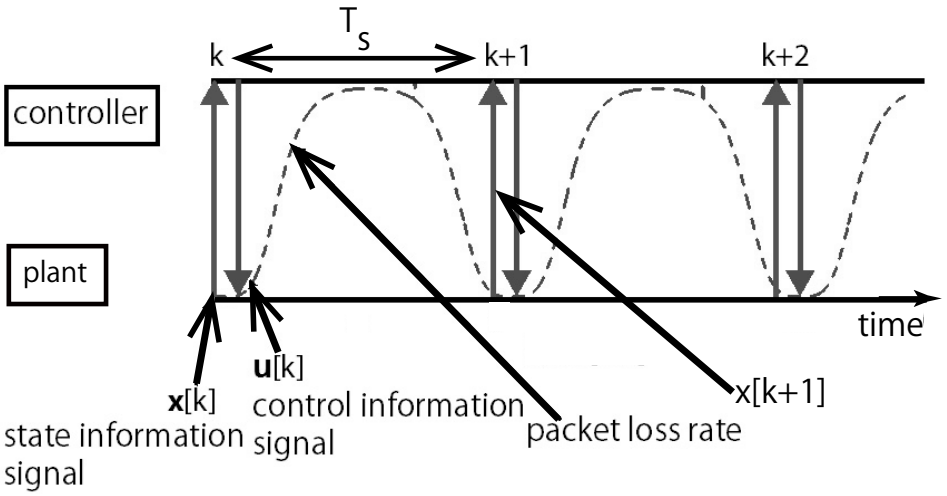

Figure 5.2 Conventional control method (low packet rate).

5.3.2 Proposed method with predictive control

Fig. 5.4 shows the behavior of the proposed system. As in Fig. 5.3, control is carried out every $T_s = 1/240$[s]. However, in the proposed system no transmissions are carried out during the instants in which $P_e[k]$ is large, in other words, when k is an odd number. On the other hand, when k is an even number, the controller sends $\mathbf{u}[k]$ and also

$$\tilde{\mathbf{u}}[k+1] = -\mathbf{K_d}\left(\mathbf{A_d}\hat{\mathbf{x}}[k] + \mathbf{B_d}\mathbf{u}[k] - \mathbf{r}[k+1]\right) \tag{5.6}$$

which is the predicted control information for the time instant $k+1$ calculated from a mathematical model, at the same time. In Eq.(5.6), the term $\mathbf{A_d}\hat{\mathbf{x}}[k] + \mathbf{B_d}\mathbf{u}[k]$ represents the predicted state information for instant $k+1$. $\mathbf{r}[k+1]$ is the future value for the reference signal $\mathbf{r}[k]$ at instant $k+1$. In this work it is assumed this future value can be known or determined by the user. In this manner, the transmission rate is 120 packets/s as in Fig. 5.2.

In this proposed system with a predictive control scheme, when k is even, its behavior is similar to that of the conventional scheme. However, when k is odd, the plant will either use the pre-calculated and previously sent next-sample value $\tilde{\mathbf{u}}[k+1]$ or $\mathbf{0}$. The algorithms are summarized as follows. In

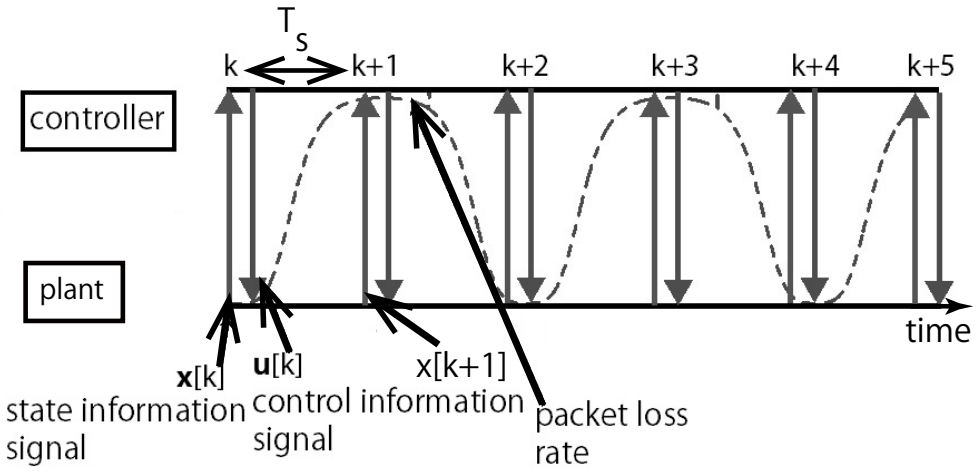

Figure 5.3 Conventional control method (high packet rate).

the plant, the estimated control signals $\hat{\mathbf{u}}[k]$ and $\hat{\mathbf{u}}[k+1]$ where k is an even number, are represented as follows:

$$\begin{cases} \hat{\mathbf{u}}[k] = \begin{cases} \mathbf{u}[k] & \text{no packet loss} \\ \mathbf{0} & \text{otherwise} \end{cases} \\ \hat{\mathbf{u}}[k+1] = \begin{cases} \tilde{\mathbf{u}}[k+1] & \text{no packet loss at instant k} \\ \mathbf{0} & \text{otherwise} \end{cases} \end{cases} . \tag{5.7}$$

The estimated signal $\hat{\mathbf{u}}[k]$ is input to the plant and the state information $\mathbf{x}[k]$ is sent back as packets to the controller also only when k is an even number. Similarly at the controller the estimated state information signal $\hat{\mathbf{x}}[k]$ where k is an even number, is given by:

$$\begin{cases} \hat{\mathbf{x}}[k] = \begin{cases} \mathbf{x}[k] & \text{no packet loss} \\ \mathbf{A_d}\hat{\mathbf{x}}[k-1] + \mathbf{B_d}\mathbf{u}[k-1] & \text{otherwise} \end{cases} \\ \hat{\mathbf{x}}[k+1] = \mathbf{A_d}\hat{\mathbf{x}}[k] + \mathbf{B_d}\mathbf{u}[k] \quad \text{always} \end{cases} . \tag{5.8}$$

5.4 Numerical Examples

In this section computer simulation methods and physical parameters for the conventional and the proposed methods are the same as in Section 4.2.

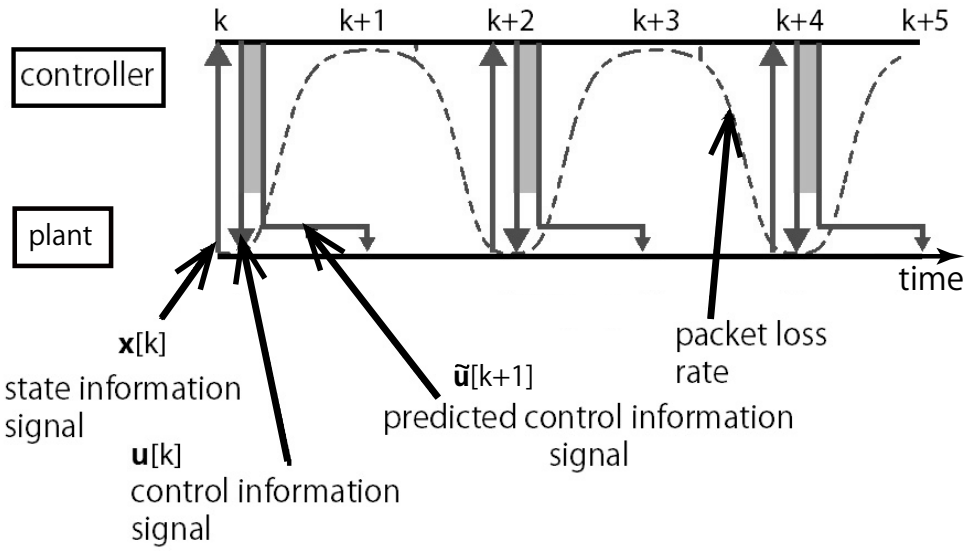

Figure 5.4 Proposed predictive control method

The simulation parameters for this Section are given in Table 5.1.

In Fig. 5.5 the bound-output stability of the system is tested by rating how many times the pendulum falls out of the given $|\theta[k]| > \frac{\pi}{6}$ range for the conventional control method and the proposed predictive control method. The tests were carried out against various levels of average signal-to-noise ratio γ and plant disturbances $\mathbf{w}[k]$ (for more details on $\mathbf{w}[k]$ see Chapter 2) of variance values: $\sigma^2_{dist} = 10^{-4}$ for the high disturbance level, and $\sigma^2_{dist} = 10^{-5}$ for the low disturbance level. The simulation trials were repeated 1000 times and each trial lasted 20 seconds.

From Fig. 5.5 it can be seen that with the high level of disturbance, the conventional method with low and high packet rates shows little difference in performance. However, the system applying the predictive control method has a better performance for low SNR levels. For the low disturbance level, the conventional method fails at very low γ values, but quickly improves. However, the system with the proposed predictive control method has a virtually perfect performance (the fall rate values lower than 10^{-3}).

In Fig. 5.6 the accuracy of control rated as the pendulum arm Root Mean

Table 5.1 Simulation parameters.

Meaning	Value
Modulation scheme	BPSK
Packet length	40 bits
Packet rates	240 and 120 packets/s
Frequency of AC signal	60 Hz
Pendulum angle target value	0 rad
Arm's period of motion	10 s
Arm angle target values	0 to π rad

Square Error (RMSE) is tested. The system applying the conventional method of control for both low and high packet rates, in general showed little difference in performance, regardless of the level of disturbance. However, even with the high level of disturbance, the proposed predictive control method showed a better performance under low SNR levels. Under the low disturbance level, the accuracy of the proposed predictive control method was better for low γ values.

It can be seen how in both Fig. 5.5 and in Fig. 5.6 the conventional and proposed schemes have a performance floor. This is due to the fact that the plant disturbance $\mathbf{w}[k]$ limits the improvements that can be achieved with better SNR levels. This tendency is shown as the values of plant disturbance variance σ^2_{dist} are decreased. In Fig. 5.7 the RMSE is evaluated for the predicted control information $\tilde{\mathbf{u}}[k+1]$ for high and low disturbance levels. The horizontal axis represents varying values of average SNR. It can be seen how the level of plant disturbance $\mathbf{w}[k]$ greatly affects the accuracy of $\tilde{\mathbf{u}}[k+1]$ and sets a performance floor that limits accuracy improvements after a certain SNR value.

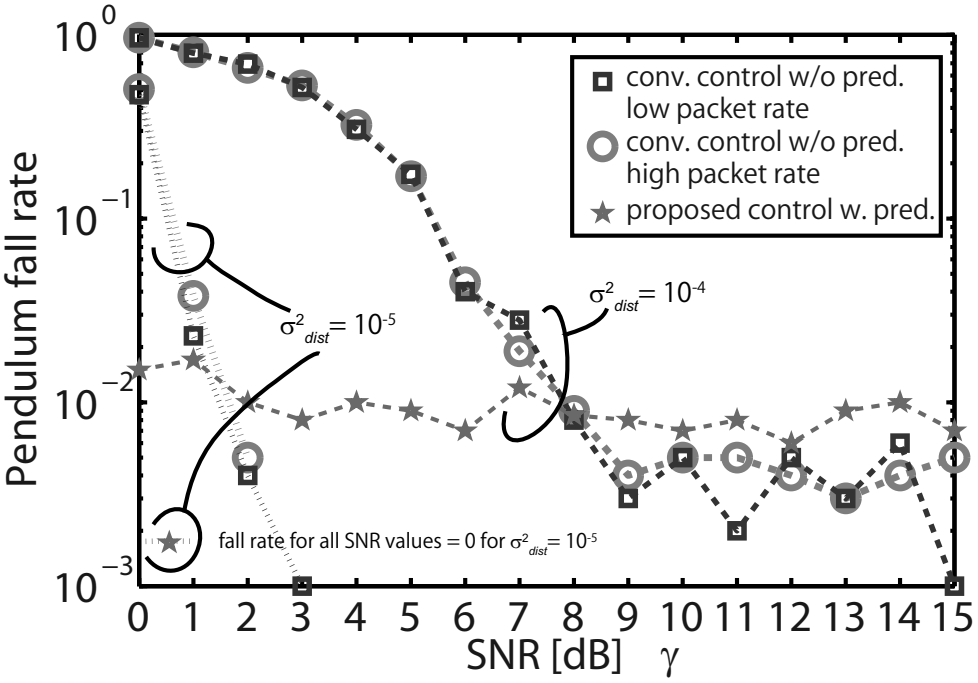

Figure 5.5 Evaluation of the pendulum fall rate for the conventional and proposed methods with varying average SNR γ and disturbance levels of variance 10^{-4} and 10^{-5}.

5.5 Summary

In this chapter it was shown how the cyclostationary features of noise can be exploited to improve the control performance of a single machine under low SNR conditions. The predictive control scheme was proven to excel at low SNR conditions in contrast to conventional methods with low and high data transmission speeds. This is due to the fact that at low SNR conditions, the delivery of correct commands in the conventional method is greatly impaired by the noise in the channel. However in the predictive method case, delivery of correct information is assured even at low SNR conditions. At high SNR conditions, the conventional methods proved to have little difference between them in the case of stability and they are both better than the predictive method when it comes to accuracy. This is mainly due to the fact that even

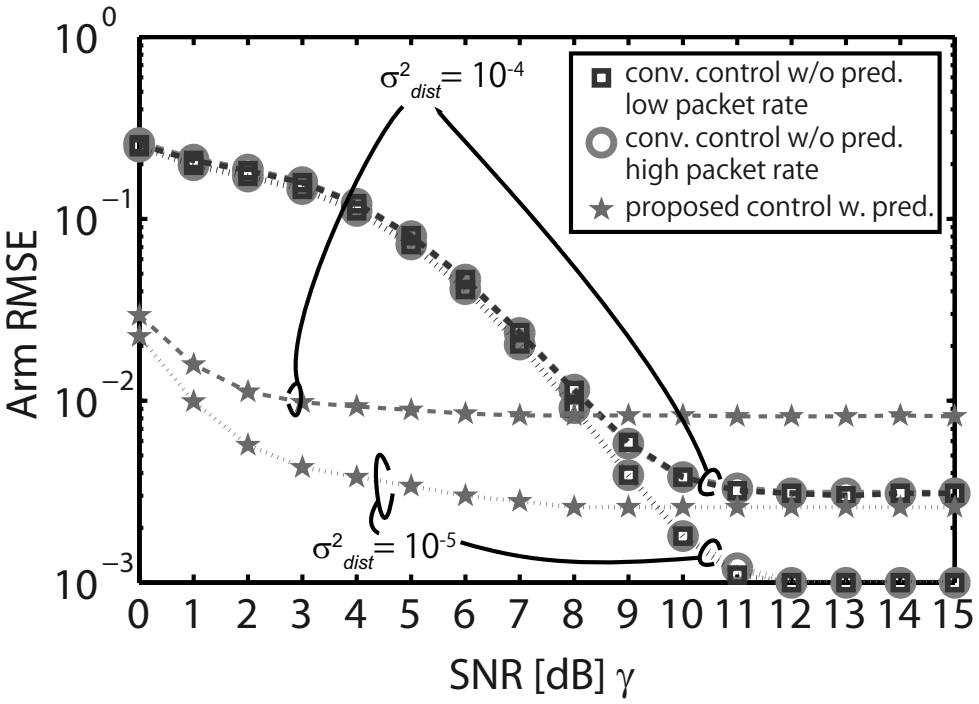

Figure 5.6 Evaluation of the arm RMSE for the conventional and proposed methods for varying average SNR γ and disturbance levels of variance 10^{-4} and 10^{-5}.

at high SNR conditions, the accuracy of the predictive method is still affected by the presence of plant disturbance. On the other hand, in the case of the conventional methods, the low noise/high SNR condition allows the delivery of the real correct information to the plant.

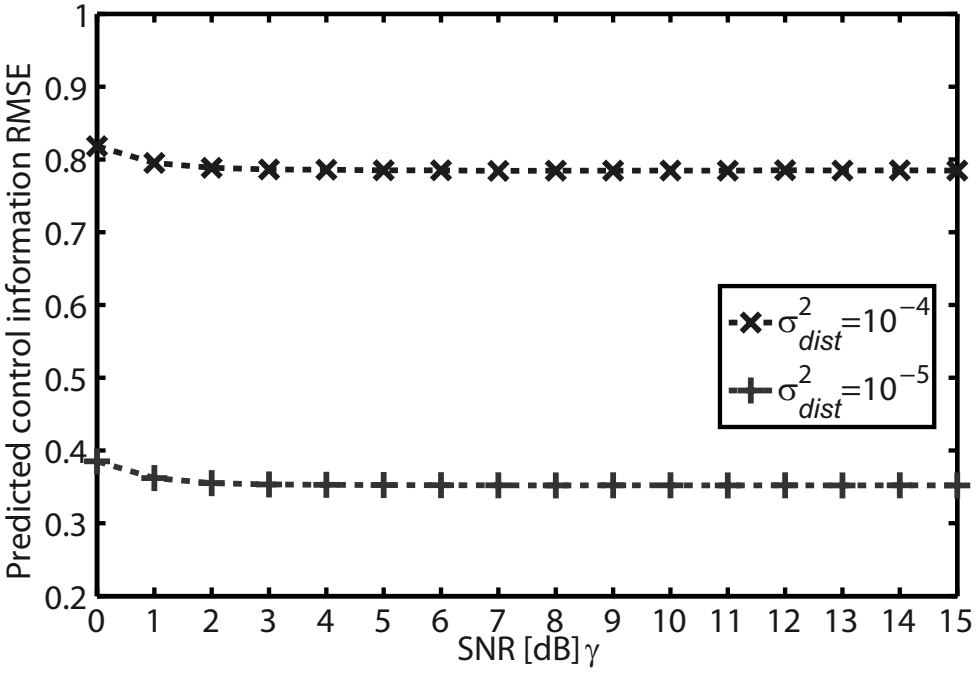

Figure 5.7 Evaluation of the predicted control information RMSE for varying average SNR γ and disturbance levels of variance 10^{-4} and 10^{-5}.

Chapter 6

Multiple machine control using narrowband PLC[44]

The ubiquity of power lines makes them considerable for applications related to the future smart grid and the control of machines in industrial environments [4]. For the realization of the future smart grid, communications for continuous sensing and control of multiple devices are very important [3]. In this research the focus is to provide improved control quality and fair medium access for multiple machine control systems sharing a power line for the communication of their control signals. There are many works on access schemes for power line communication (PLC) systems. For example, [26] employs intelligent time division multiple access (TDMA) to offer broadband access to various devices sharing home power line communications. In [27], orthogonal frequency division multiple access (OFDMA) along with a proposed carrier-sense multiple access and a collision-avoidance (CSMA/CA) protocol considering channel condition are applied. However, in none of the previous works, the issue of fair medium access for multiple machine control in narrowband power line communications has been addressed.

In this chapter, multiple machine feedback control systems sharing a power line serving as the feedback loops between the controller and the plants are considered. The noise and attenuation in the power line are assumed as cyclo-

stationary [25],[38], therefore the signal-to-noise ratio (SNR) and the bit error rate (BER) are also cyclic.

6.1 Feedback control system for multiple machines

Fig. 6.2 shows a general layout of a discrete-time feedback control system with a power line used for its feedback loops. In this system M plants are controlled. In the system, the discrete state information at time instant $t = kT_D$, $\mathbf{x}_m[k]$ is transmitted from the m-th plant to the controller and the discrete control information $\mathbf{u}_m(k+1)$ is sent back as packets from the controller to the plant m at $t = (k+1)T_D$, where T_D is a constant value, k is an integer, and $m = 1, 2, ...M$. In Fig. 6.2, TX denotes a transmitter and RX is a receiver. If there are no errors in the PLC channel, the output of RX on the plant side $\hat{\mathbf{u}}_m[k]$ is identical to $\mathbf{u}_m[k]$ and the output of RX on the controller side $\hat{\mathbf{x}}_m[k]$ is $\mathbf{x}_m[k]$. If at least a one-bit error occurs in a packet, RX discards the received packet and calculates a substitute value as described in Section 6.3.1.

As an example of each plant, a rotary inverted pendulum that requires feedback control for its proper operation [8] is employed. Details on the pendulum's physical properties are the same as in Chapter 5, however the explanation for the multiple machine case is shown below. The pendulum's rod mass is defined as M_p, and the rod's length is defined as L. The pendulum's arm length is R and the arm's central moment of inertia is defined as J_b. In Fig. 6.1, $\theta_m[k]$ and $\phi_m[k]$ are defined as the angles of the pendulum and the arm. The digital state information is denoted as:

$$\mathbf{x}_m[k] = [\ \theta_m(t) \quad \phi_m(t) \quad \dot{\theta}_m(t) \quad \dot{\phi}_m(t)\ ]^T \tag{6.1}$$

of the m-th rotary inverted pendulum at time instant $t = kT_D$. The objective of the control is to make $\mathbf{x}_m[k]$ follow the reference vector function $\mathbf{r}_m[k]$. In

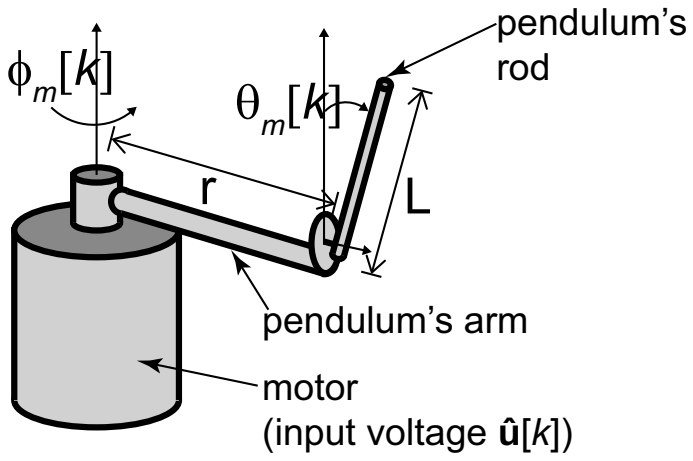

Figure 6.1 Basic structure of the rotary inverted pendulum considered in this work.

order to achieve this objective, the controller calculates the necessary input value, or the voltage to the motor $\mathbf{u}_m[k]$. Further details on the behavior of the plant and the derivation of $\mathbf{u}_m[k]$ are given in Section 6.3.1 and in Chapter 2.

6.2 Communication Quality of Time Slots

As in Chapters 3, 4 and 5, the noise is assumed to be the dominant factor for the cyclic features of communication quality and its SNR is $1/\hat{\sigma}^2(t)$ where $\hat{\sigma}^2(t)$ is the noise power as a time function. The SNR is also assumed to be constant throughout the duration of each packet.

Under the above assumption, in [38], the model for the PER is derived at $t = kT_D$ in Eq. (5.1) where the BER considering BPSK modulation is Eq.(5.2) and the noise power is Eq. (5.3) based on the noise model of [25].

According to Eq. (5.1) and Eq. (5.3), the behavior in the channel theoretically repeats every $T_{AC}/2$. This periodic behavior of noise and the fact that in machine control high data rate is not such a critical factor, allow the implementation of Time Division Multiple Access to assign time slots to each machine.

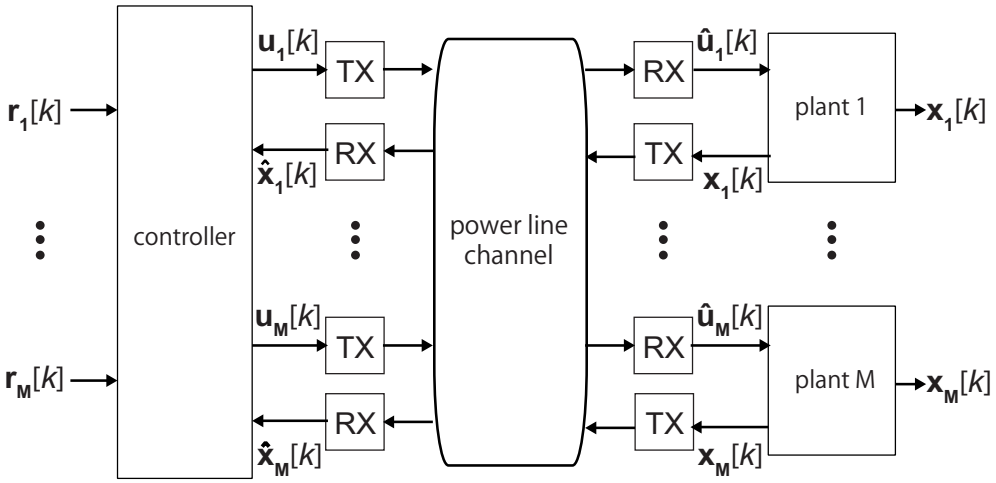

Figure 6.2 Block diagram of a discrete multiple machine control system with a power line as the feedback loops.

This division into time slots of varying qualities is illustrated in Fig. 6.3.

Each period of cyclostationary noise is named as a frame and each frame is further subdivided into $2M$ time slots, each with a different quality. The duration of each slot is $T_D = \frac{T_{AC}/2}{2M} = \frac{T_{AC}}{4M}$. In the next sections, the assignment of these slots will be further explained.

6.3 Medium access for multiple machine control in PLC

After receiving $\hat{\mathbf{x}}_m[k]$, the controller calculates discrete control information and sends it back to the m-th plant in the next slot as $\mathbf{u}_m[k+1]$, hence two time slots are necessary for this pair of packets. Since each frame has $2M$ slots, each machine gets a pair of slots assigned to it in each frame. This section describes two schemes of assignment.

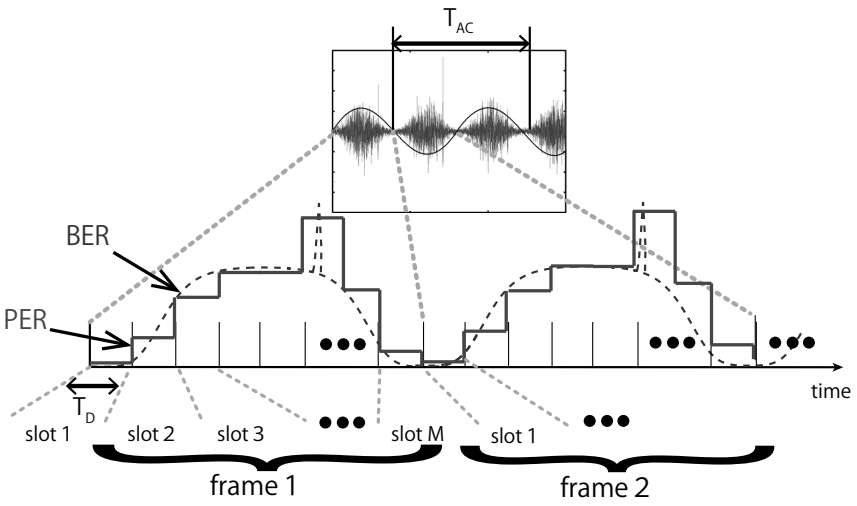

Figure 6.3 Quality of time slots

6.3.1 Fixed Time Slot Assignment Scheme

In the case of the fixed time slot assignment scheme, a pair of state and control information packets are transmitted once a frame with the fixed interval $2MT_D$. We define the order of this pair of state and control information packets in the frame as S. In the case of the fixed time slot assignment scheme, $S = m$. We must also define the frame number $f = \lfloor t/(2MT_D) \rfloor$ and $k = 2Mf + 2S$. Thus if a plant sends data in the k-th slot, the next transmission is at $t = (k + 2M)T_D$. In other words, the location of a pair of time slots assigned to each plant is fixed in a frame in position $S = m$ as in Fig. 6.4. In our model we do not consider transmission delays, therefore the arrows that represent packet transmissions are perfectly vertical.

The state information of the m-th plant is sent to the controller in the k-th slot, then the output of RX on the controller side, or the estimated state information signal is given by:

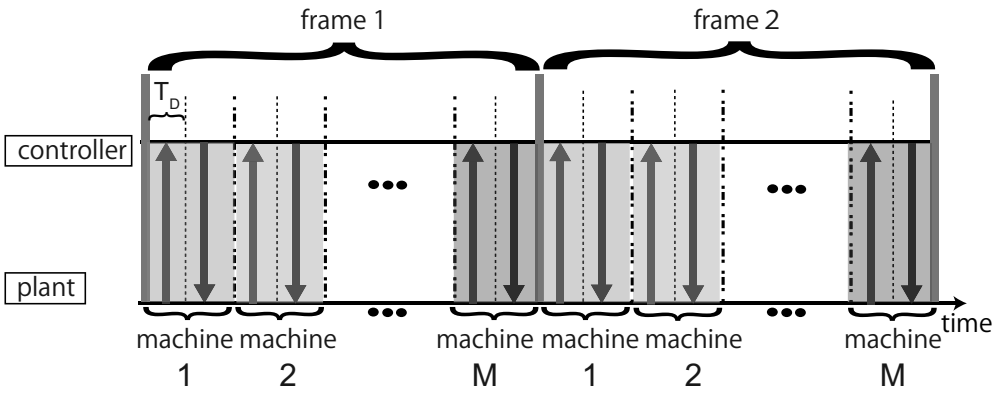

Figure 6.4 Fixed time slot assignment for M machines.

$$\hat{\mathbf{x}}_m[k] = \begin{cases} \mathbf{x}_m[k] & \text{no packet loss} \\ \mathbf{A_d}\hat{\mathbf{x}}_m[k-2M] & \\ +\mathbf{B_d}\mathbf{u}_m[k-2M+1] & \text{otherwise} \end{cases} . \tag{6.2}$$

Details on the vectors $\mathbf{A_d}$ and $\mathbf{B_d}$ are shown in the Appendix.

After having $\hat{\mathbf{x}}_m[k]$ the controller calculates the control information and sends it to the m-th plant in the $(k+1)$-th slot. At the plant side, RX output, or the estimated control signal is represented as:

$$\hat{\mathbf{u}}_m[k+1] = \begin{cases} \mathbf{u}_m[k+1] & \text{no packet loss} \\ \mathbf{0} & \text{otherwise} \end{cases} . \tag{6.3}$$

This estimated signal $\hat{\mathbf{u}}_m[k]$ is input to the plant, at $t = (k+1)T_D$.

6.3.2 Cyclic Time Slot Assignment Scheme

In the case of the cyclic time slot assignment scheme, a pair of state and control information packets are transmitted once a frame with varying intervals. The frame number f and k are defined as in the fixed time slot assignment scheme. However, for the cyclic time slot assignment scheme, the order of the pair of state and control information packets in the frame is S =

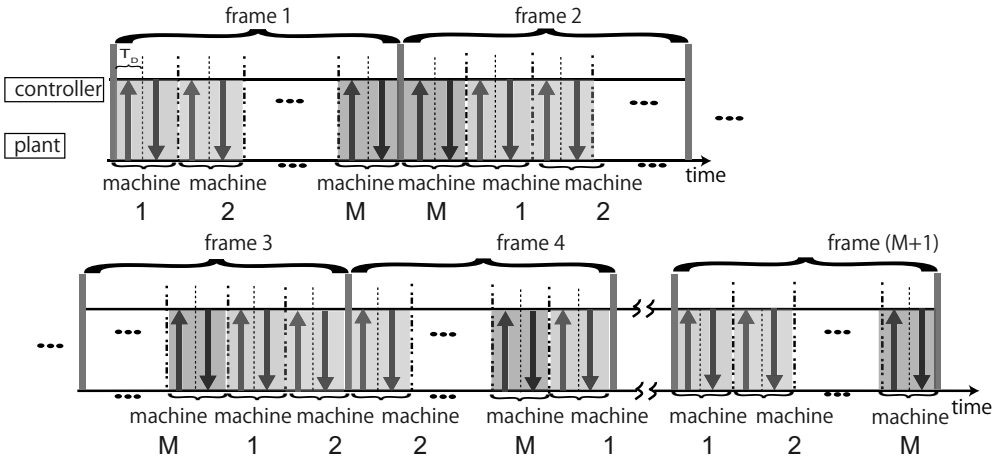

Figure 6.5 Cyclic time slot assignment for M machines.

mod $(m + f, M)$. In this way the position of a pair of time slots assigned to each plant is cycled as shown in Fig. 6.5.

The state information of the m-th plant is sent to the controller in the k-th slot, then the output of RX on the controller side, or the estimated state information signal $\hat{\mathbf{x}}_m[k]$ and $\hat{\mathbf{u}}_m[k+1]$ are calculated as in the fixed assignment scheme in Eq.(6.2) and (6.3), however, the intervals between commands are not fixed.

6.4 Numerical Examples

The control quality of the system, or in other words the ability of the plant to keep its stability as well as to accurately follow desired values is evaluated, to know the performance of the system.

In this the fixed and the cyclic assignment schemes are simulated and then

the stability and control accuracy of each system is compared. The settings for the simulations performed are the same used in Section 4.2.

A very low value is used for the plant disturbances $\mathbf{w}[k]$ variance $\sigma^2_{dist} = 10^{-8}$. The simulation trials were repeated 50 times and each trial lasted 25 seconds.

From Fig. 6.6 it can be seen that the performance for machine 1 is better than that of machine 2 and machine 3. Also, the performance of machine 2 is the worst among the three. This behavior is due to the fact that all machines fall under the same slots every frame, and each slot has a probability of error that virtually repeats itself in each frame. This is caused by the cyclic communication quality feature of PLC. From Fig. 6.7 it can be seen how the performance of all machines is approximately the same regardless of the SNR level. This is due to the fact that all machines make use of the slots in a fair manner. The influence of variable intervals between control commands is not noticeable.

In Fig. 6.8 and Fig. 6.9 the accuracy of control is rated as the Root Mean Square Error (RMSE) of the angle of the pendulum arm that is affected by errors in the communication channel and disturbance, against the no channel error and no disturbance case. The system applying the fixed assignment scheme shows us that machine 2 has a very bad performance when compared to machine 1 and machine 3. In the system applying the cyclic assignment scheme it is seen that for low SNR values the performance for most machines is a little worse than for machine 3 in the fixed assignment system. This is due to the influence of the variable command timing intervals in the cyclic assignment scheme. However, in this system all machines show approximately the same behavior.

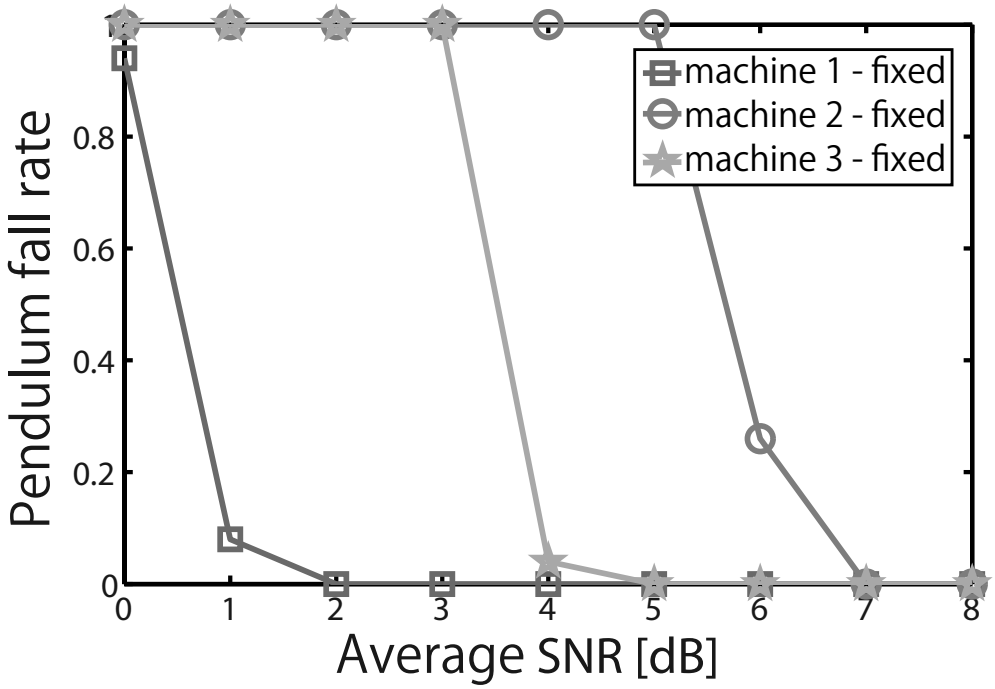

Figure 6.6 Evaluation of the pendulum fall rate for the three machines for the fixed slot assignment scheme for varying SNR γ.

6.5 Summary

In this chapter, the performance of a control system that is influenced by the cyclic packet losses in power line communication channels connecting its controller and plants, was evaluated. The fixed time slot assignment method, showed a very bad stability performance for some of the plants in comparison to the cyclic time slot assignment scheme, in which all plants showed a similar stability. In the case of the accuracy, we could see that there was an improvement for some plants for the case of the cyclic time slot assignment scheme, however the effect of the variable timing of the control commands is notable. This proves that a cyclic slot assignment scheme provides fair access to all machines, but not necessarily good quality of control.

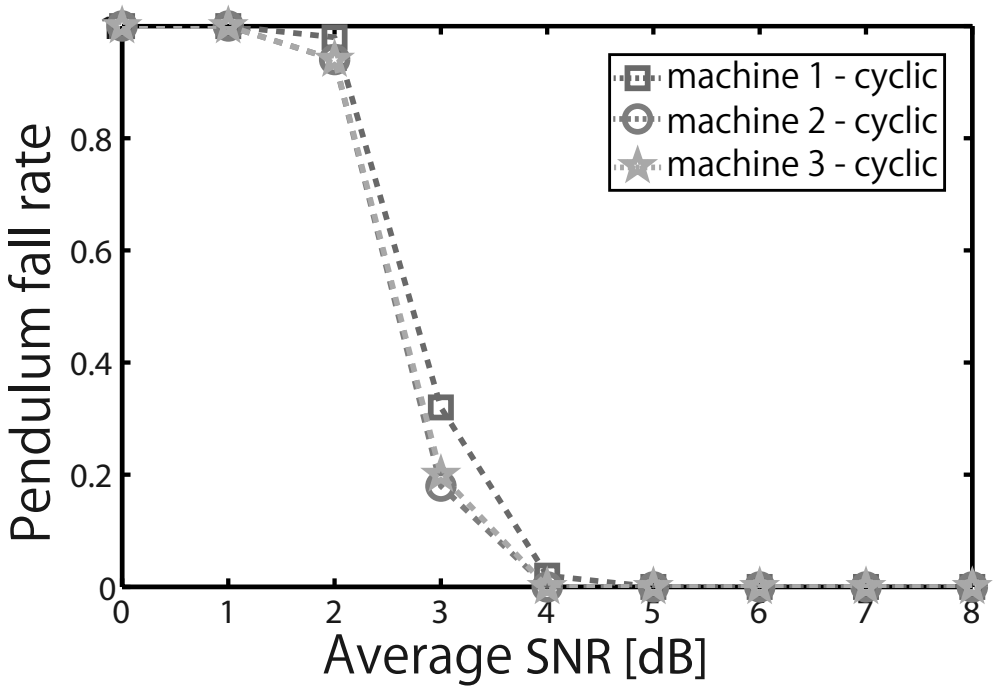

Figure 6.7 Evaluation of the pendulum fall rate for the three machines for the cyclic slot assignment scheme for varying average SNR γ.

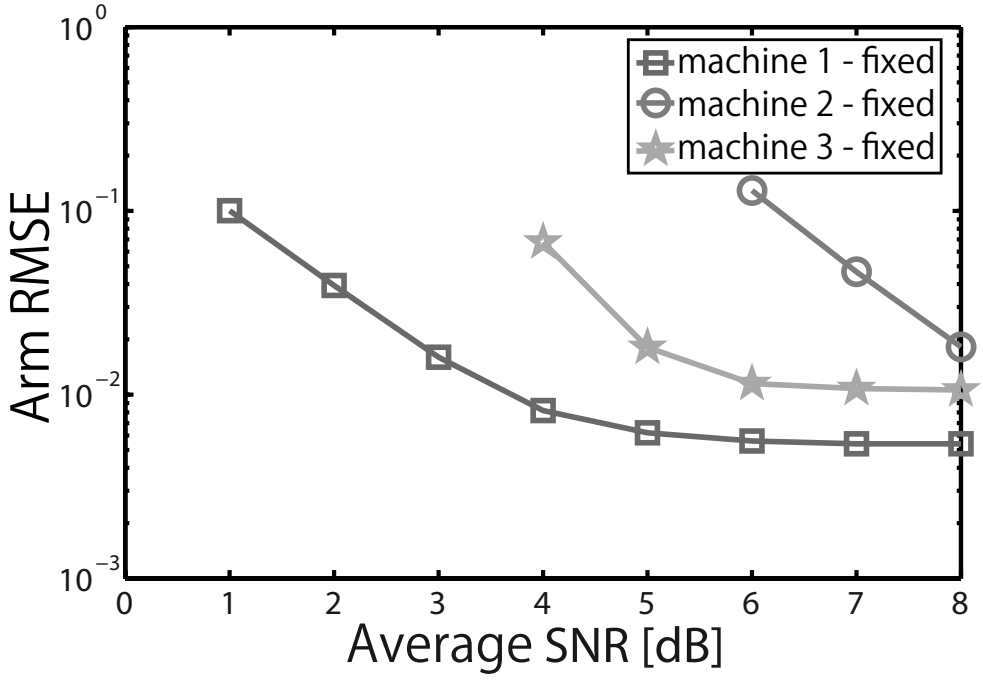

Figure 6.8 Evaluation of the arm RMSE for the three machines for the fixed slot assignment scheme for varying SNR γ.

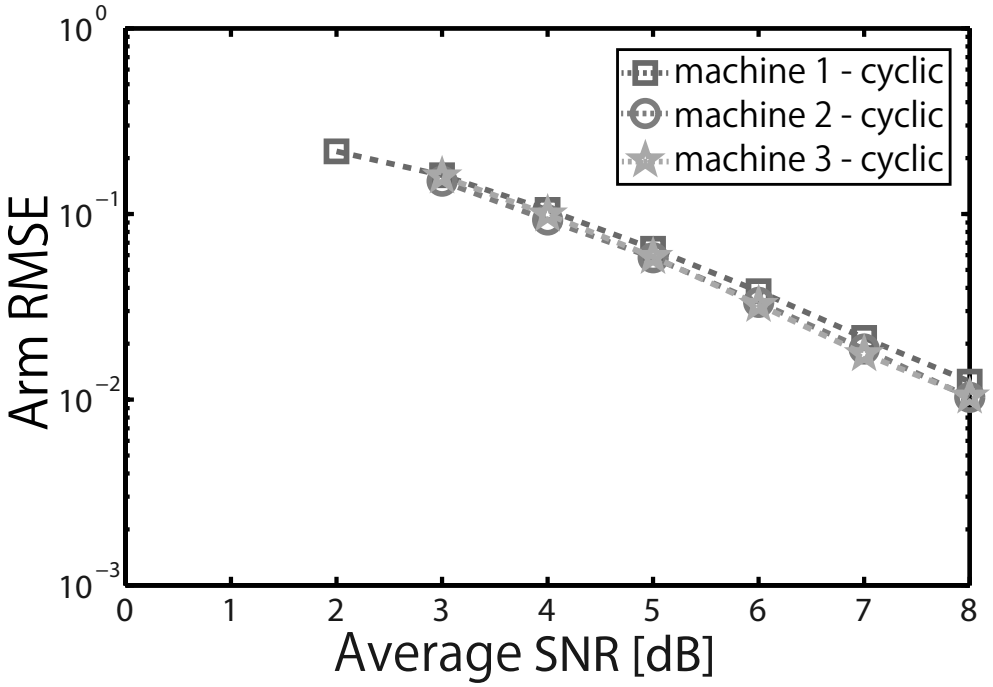

Figure 6.9 Evaluation of the arm RMSE for the three machines for the cyclic slot assignment scheme for varying average SNR γ.

Chapter 7

Conclusion

7.1 Summary of the dissertation

In this research, the influence of packet losses in a feedback control system using narrowband power line communication was explored. Narrowband power line communication presents advantages such as longer propagation distances and less interference when compared to broadband power line communications. This is beneficial as it eases its application to control indoors and outdoors (for industrial environments or the smart grid for example). However, narrowband sets limitations on the data rate which can be achieved, therefore the efficient use of the medium is necessary. Additionally, PLC in general presents cyclostationary features in its noise and attenuation, and such a structure in the noise proved to be beneficial in the application of a predictive scheme.

In this study it was proven in Chapter 4 there is indeed an advantage in the application of feedback control in a narrowband power line environment under low SNR conditions. At low SNR conditions, the cyclostationary environment allows for more correct information to be delivered to the plant than in the stationary case. This fact sets a precedent for the exploitation of this feature in Chapter 5 through the use of predictive control. Predictive control however, presents limitations in its accuracy due to disturbances in the plant. This fact

is unavoidable and becomes specially evident at high-SNR/high-disturbance levels when the non-predictive methods achieve a better performance. It was shown that from the communication viewpoint there is a limit in the improvements that can be made and a more thorough cooperation with control theory techniques is neccessary.

To extend the application of the system to reality, an introduction to multiple machine control through PLC is presented in Chapter 6. The nature of control signals with transmission rates which are relatively low allows for the application of periodic Time Division Multiple Access to serve various machines. However, the existence of different quality time slots in the cyclostationary environment requires a fair method to offer access and good control quality to all machines. Fair access is achieved by assigning time slots to each machine in a cyclic fashion, unfortunately this does not necessarily assure good control quality.

As an overall conclusion, this study proved that neither control theory by itself nor communication theory by itself can solve all the issues of a feedback control system which considers channel and plant disturbances. Improvements from the communication viewpoint were achieved, however a clear limit was reached and shown in Chapter 5 and again in Chapter 6.

7.2 Future developments

Throughout this work it was demonstrated that a feedback control system which is affected by both channel and plant disturbances may require the cooperation of both control and communication theory. From the control point of view, the use of a more sophisticated controller may help mitigate the effects of disturbances in the plant [37]. From the communication point of view, it was shown in Chapter 5 that there is a limit on how much improvement can be achieved considering the presence of these plant disturbances. In Chap-

ter 6 it was also shown that a rearrangement for the access of machines to the communication medium is not enough to assure good control quality, however fairness can be assured. To assure such fairness, a single-slot cyclic shifting scheme to access the medium was proposed, however it is understood that if the number of machines increases, a single-slot shift may not suffice. To optimize this system, it is necessary to find an optimal value of slots to shift based on the number of machines. To achieve further improvements, a more sophisticated scheme integrating a better controller together with the observation of the state of the plant to offer communication priority may be the key.

Reference

[1] N. Elia "When Bode meets Shannon: control-oriented feedback communication schemes," IEEE Transactions on Automatic Control vol. 49, pp. 1477-1488, Sept. 2004

[2] S. Galli and A. Scaglione and Z. Wang "For the Grid and Through the Grid: The Role of Power Line Communications in the Smart Grid," Proceedings of the IEEE vol. 99, pp. 998–1027, June 2011

[3] W. Liu and M. Sigle and K. Dostert "Channel Characterization and System Verification for Narrowband Power Line Communication in Smart Grid Applications," IEEE Communications Magazine, vol. 49, pp. 28–35, December 2011

[4] G. Bumiller and L. Lampe and H. Hrasnica, "Power Line Communication Networks for Large-Scale Control and Automation Systems," IEEE Communications Magazine, vol. 48, pp. 106-113, April 2010

[5] N. Ginot and M. Mannah and C. Batard and M. Machmoum, "Application of Power Line Communication for Data Transmission Over PWM Network," IEEE Transactions on Smart Grid, vol. 1, pp. 178-185, Sept. 2010

[6] H. Ferreira and L. Lampe and J. Newbury and T. Swart, "Power Line Communications Theory and Applications for Narrowband and Broadband Communications over Power Lines,"Wiley, 2010

[7] M. Nagahara and D. Quevedo and J. Ostergaard “Sparse Packetized Predictive Control for Networked Control over Erasure Channels,” IEEE Transactions on Automatic Control vol. 59, pp. 1899-1905, July 2014

[8] N. Ploplys, “Wireless Feedback Control of Mechanical Systems,” Department of Mechanical Engineering, University of Illinois, Champaign, IL, 2003

[9] T. Kondo and K. Kobayashi and M. Katayama, “A Wireless Cooperative Motion Control System with Mutual Use of Control Signals,” 2011 International Conference on Intelligent Computing and Information Technology (ICIT2011), pp.33-38, 2011

[10] R. Kohinata, “Evaluation of the Influence of Transmission Errors on the Quality of a Wireless Control System,” Department of Electrical Engineering and Computer Science, Graduate School of Engineering, Nagoya University, 2009

[11] K. Furuta and M. Yamakita and S. Kobayashi “Swing up Control of Inverted Pendulum,” 1991 IEEE International Conference on Industrial Electronics, Control and Instrumentation vol. 3, pp. 2193-2198, Nov. 1991

[12] M. Nassar and J. Lin and Y. Mortzavi and A. Dabak and I. Kim and B. Evans “Local Utility Power Line Communications in the 3-500 kHz Band,” IEEE Signal Processing Magazine vol. 29, pp. 116-127, Sept. 2012

[13] S. Hsieh and T. Ku and J. Tsai and C. Lin and C. Chen “Broadcasting control of intelligent air conditioners using power line carrier technology,” 2014 IEEE Industrial and Commercial Power Systems Technical Conference pp. 1-6, May 2014

[14] M. Samarawickrama and K. Pathirage, and H. Samarasekara and A. Wickramasinghe and K. Samarasinghe “Power Line Intercom - narrowband voice communication over power line,” International Conference on Industrial and Information Systems (ICIIS) pp. 37-42, Dec. 2009

[15] V. Oksman and J. Zhang “G.HNEM: The New ITU-T Standard on Narrowband PLC Technology,” IEEE Communications Magazine vol. 49, pp. 36-44, Dec. 2011

[16] B. Baraboi “Narrowband Powerline Communication Application and Challenges,” Ariane Controls Inc. March 2013

[17] J. Meng “Noise Analysis of Power-Line Communications Using Spread-Spectrum Modulation,” IEEE Transactions on Power Delivery vol. 22, pp.1470-1476, July 2007

[18] V. Degardin, M. Lienard, P. Degauque “Transmission on indoor power lines: from a stochastic channel model to the optimization and performance evaluation of multicarrier systems,” Int. J. Commun. Syst. vol. 16, pp. 363-379, April 2003

[19] N. Pavlidou. A. J. H. Vinck, J. Yazdani, B. Honary “Power line communications: State of the art and future trends,” IEEE Communication Magazine vol. 41, pp. 34-40, April 2003

[20] F. Canete, J. Cortes, L. Diez, J. Entrambasaguas “Analysis of the cyclic short-term variation of indoor power line channels,” IEEE Journal on Selected Areas in Communications vol. 24, pp. 1327-1338, July 2006

[21] M. Nassar, A. Dabak, I. H. Kim, T. Pandle, B. L. Evans “Cyclostationary noise modeling in narrowband powerline communication for smart grid applications,” Proc. IEEE Int. Conf. Acoustics, Speech, and Signal Processing, pp. 3089-3092, March 2012

[22] D. Rieken “Periodic noise in very low frequency power-line communications,” Proc. IEEE Int. Symp. Power Line Communications and Its Applications pp. 295-300, 2011

[23] M. Zimmerman, K. Dostert “Analysis and modeling of impulsive noise in broad-band powerline communications,” IEEE Transactions on Electromagnetic Compatibility vol. 44, pp. 249-258, February 2002

[24] D. Middleton “Statistical-physical models of electro-magnetic interference,” IEEE Transactions on Electromagnetic Compatibility vol. EMC-19, pp. 106-126, August 1977

[25] M. Katayama and T. Yamazato and H. Okada “A Mathematical Model of Noise in Narrowband Power Line Communication Systems,” IEEE Journal on Selected Areas in Communications, vol. 24, pp. 1267–1276, July 2006

[26] S. Ohmi and S. Yoshida and T. Yamaguchi and G. Kuroda ”A Media Access Control Method for High-speed Power Line Communication System Models,” 2004 First IEEE Consumer Communications and Networking Conference pp. 295–300, January 2004

[27] S. Yoon and D. Kang and S. Bahk “Multichannel CSMA/CA Protocol for OFDMA-Based Broadband Power-Line Communications,” IEEE Transactions on Power Delivery vol. 28, pp. 2491–2499, October 2013

[28] T. Smailian, F. Kschiechang, P. Gulak “In-building power lines as high-speed communication channels: channel characterization and a test channel ensemble,” Int. J. Commun. Syst., vol. 16, pp. 381-400, May 2003

[29] D. Anastasiadou, T. Antonakopoulos “Multipath characterization of indoor power-line networks,” IEEE Transactions on Power Delivery vol. 20, pp. 90-99, January 2005

[30] N. Sawada and T. Yamazato and M. Katayama “Bit and Power Allocation for Power-Line Communications under Nonwhite and Cyclostationary Noise Environment,” IEEE International Symposium on Power Line Communications and its Applications 2009

[31] A. Perez and A. Sanchez and J. Regue and M. Ribo and R. Aquilue and P. Rodriguez-Cepeda and F. Pajares “Circuital and Modal Characterization of the Power-Line Network in the PLC Band,” IEEE Transactions on Power Delivery, vol. 24, pp. 1182–1189, July 2009

[32] Z. Wang and A. Scaglione and R. Thomas “Generating Statistically Correct Random Topologies for Testing Smart Grid Communication and Control Networks,” vol. 1, pp. 28–39, June 2010

[33] G. Srinivasa Prasanna and A. Lakshmi and S. Sumanth and V. Simha and J. Bapat and G. Koomullil “Data Communication over the Smart Grid,” 2009 IEEE International Simposium on Power Line Communications and Its Applications pp. 273–279, March 2009

[34] K. Ko and M. Kim and K. Bae and D. Sung and J. Kim and J. Ahn “A Novel Random Access for Fixed-Location Machine-to-Machine Communications in OFDMA Based Systems,” IEEE Communications Letters vol. 16, pp. 1428–1431, September 2012

[35] J.Proakis, Digital Communications Fifth Edition, McGrawHill, 2008.

[36] A. Oppenheim and R. Schafer, “Discrete-Time Signal Processing Third Edition,” Prentice Hall, 2010

[37] K. Zhou and J. Doyle and K. Glover, “Robust and Optimal Control,” Prentice Hall, 1996

[38] C. Carrizo and K. Kobayashi and H. Okada and M. Katayama “Control Quality of a Feedback Control System Under Cyclostationary Noise in

Power Line Communication," IEICE Transactions on Fundamentals vol. E95-A, pp. 706-712, April 2012

[39] C. Carrizo and K. Kobayashi and H. Okada and M. Katayama, "Influence of Cyclostationary Noise on the Behavior of a Powerline-controlled Rotary Inverted Pendulum," Technical Report of IEICE, RRRC2011-6, pp. 19-24, June 2011.

[40] C. Carrizo, K. Kobayashi, H. Okada, M. Katayama, "Evaluation of the influence of cyclostationary noise in a power line on the control quality of a rotary inverted pendulum," Engineering Sciences Society Conference of IEICE, AS-2-5, pp.S-11 - S-12, Sept. 2011

[41] C. Carrizo and K. Kobayashi and H. Okada and M. Katayama, "Feedback control scheme with prediction for power line communication channels," 2013 IEEE International Conference on Smart Grid Communications pp. 289–293, October 2013

[42] C. Carrizo, K. Kobayashi, H. Okada, M. Katayama, "Predictive Control for Performance Improvement of a Feedback Control System using Cyclostationary Channels," IEICE Transactions on Fundamentals, accepted (2014)

[43] C. Carrizo, K. Kobayashi, H. Okada, M. Katayama, "Performance Improvement of a Feedback Control System in a Power Line Environment through the use of a Cyclostationary Noise-Adapted Predictive Control Scheme," IEICE General Conference, AS-3-8, pp.S-36 - S-37, March 2013

[44] C. Carrizo, K. Kobayashi, H. Okada, M. Katayama, "A Study of Time Division Multiple Access Schemes for the Control of Machines using Narrowband Power Line Communication," IEICE Technical Report, RCC2014-24, pp.13-18, July 2014

Acknowledgements

Initially I would like to thank my family, in special my mother and my father for their remote support and encouragement at all times. Without them I would have not been able to fulfill my life in Japan and carry on through the difficult moments. I would like to express my sincere gratitude to my advisor, Dr. Masaaki Katayama, Professor of EcoTopia Science Institute, Nagoya University, Japan. His very valuable guidance and encouragement were essential to carry out my research work. Professor Katayama not only guided me through the professional path, but also as a human being by offering me fundamental and very clever advices to succeed in life. I learned from him the importance of manners, discipline and consistency, to be applied not only when carrying out research work, but also in other aspects of life as well. I also believe professor Katayama's deep knowledge together with his great patience are truly admirable features in his character. Thanks to him I felt the constant need to move forward and not give up my path to excellency and the mastery of knowledge. I would also like to thank Dr. Takaya Yamazato, Professor of the Institute of Liberal Arts and Sciences, Nagoya University, Japan, for his warmth, friendliness and sincere comments. Additionally I want to thank Dr. Hiraku Okada, Associate Professor of EcoTopia Science Institute, Nagoya University, Japan, for his accurate and very concrete advices and corrections to my work. I feel that I am also in great debt to professor Kentaro Kobayashi for his kindness, patience, and dedicated support towards me at various times throughout my life as a researcher in Katayama Laboratory. Without his essential guidance, I probably would not have been able to overcome

the various technical and conceptual difficulties which arose throughout my experiments. Professor Kobayashi was always there available at almost any time and would always help me with a lot of promptness and enthusiasm. All his help was crucial in the production of works with a clear and logical structure that would make them easier to understand by many readers. I sincerely want to thank Dr. Shinji Doki, Professor of Graduate School of Engineering, Nagoya University, Japan, for cooperating with his expertise in control theory and his valuable comments through a crucial phase in the development of this work. I must also thank Dr. Shinsuke Hara, Professor of the Graduate School of Engineering, Osaka City University, Japan, for his valuable suggestions applied in the creation of this work and the comments I received from him in the various conferences and academic gatherings in which I had the pleasure to meet him. Katayama laboratory's technical staff Mr. Yoshihiko Kito and Katayama laboratory's administrative staff Mrs. Aiko Ishikawa and Mrs. Eriko Shiraishi also supported me greatly so I would like to deeply thank them as well. I believe it is worthy to mention the support I received from all my seniors, in special Jan Zaleski, Jun Naganawa, Tsugunori Kondo and Fumikazu Minamiyama. They provided me with very important references and initial information which served as a base and a kickstart to my research work. Last but not least, I would like to thank the many friends I have made throughout my stay in this wonderful country. In one way or another they influenced me to improve, strengthen my character and overcome the bad times without turning back even once.

Research publications

I. Journal papers

1. C. Carrizo, K. Kobayashi, H. Okada, M. Katayama, “Control Quality of a Feedback Control System Under Cyclostationary Noise in Power Line Communication,” IEICE Transactions on Fundamentals, vol. E95-A, no.4, pp.706-712, April 2012

2. C. Carrizo, K. Kobayashi, H. Okada, M. Katayama, “Predictive Control for Performance Improvement of a Feedback Control System using Cyclostationary Channels,” IEICE Transactions on Fundamentals, vol. E98-A, no.4, April 2015

*IEICE: The Institute of Electronics, Information and Communication Engineers

II. International Conference

1. C. Carrizo, K. Kobayashi, H. Okada, M. Katayama, “Feedback Control Scheme with Prediction for Power Line Communication Channels,” IEEE International Conference on Smart Grid Communications, pp.289-293, October 2013

*IEEE: The Institute of Electrical and Electronics Engineers

III. National Conferences

1. C. Carrizo, K. Kobayashi, H. Okada, M. Katayama, "Influence of Cyclostationary Noise on the Behavior of a Powerline-controlled Rotary Inverted Pendulum," IEICE Technical Report, RRRC2011-6, pp. 19-24, June 2011.

2. C. Carrizo, K. Kobayashi, H. Okada, M. Katayama, "Evaluation of the influence of cyclostationary noise in a power line on the control quality of a rotary inverted pendulum," Engineering Sciences Society Conference of IEICE, AS-2-5, pp.S-11 - S-12, Sept. 2011

3. C. Carrizo, K. Kobayashi, H. Okada, M. Katayama, "Performance Improvement of a Feedback Control System in a Power Line Environment through the use of a Cyclostationary Noise-Adapted Predictive Control Scheme," IEICE General Conference, AS-3-8, pp.S-36 - S-37, March 2013

4. C. Carrizo, K. Kobayashi, H. Okada, M. Katayama, "A Study of Time Division Multiple Access Schemes for the Control of Machines using Narrowband Power Line Communication," IEICE Technical Report, RCC2014-24, pp.13-18, July 2014